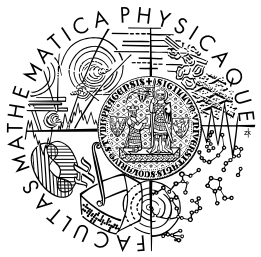

FACULTY
OF MATHEMATICS
AND PHYSICS
Charles University

MASTER THESIS

Ondřej Kincl

Thermodynamic modelling of rolling fluid turbine

Mathematical Institute of the Charles University

Supervisor of the master thesis: RNDr. Michal Pavelka, Ph.D.

Study programme: Mathematical Modelling in Physics and Technology

Study branch: Continuum Mechanics

Prague 2020

I declare that I carried out this master thesis independently, and only with the cited sources, literature and other professional sources. It has not been used to obtain another or the same degree.

I understand that my work relates to the rights and obligations under the Act No. 121/2000 Sb., the Copyright Act, as amended, in particular the fact that the Charles University has the right to conclude a license agreement on the use of this work as a school work pursuant to Section 60 subsection 1 of the Copyright Act.

In ..... date ....

Author's signature

I would like to thank my supervisor RNDr. Michal Pavelka, Ph.D. and my consultant prof. Ing. František Maršík, DrSc. for their great patience and enthusiasm, which was very inspirational for me and made writing this thesis possible. I am also grateful that I was able to meet with Doc. Ing. Miroslav Sedláček CSc., who shared his great experience with me and provided me working models of the turbine for experiments.

Title: Thermodynamic modelling of rolling fluid turbine

Author: Ondřej Kincl

Institute: Mathematical Institute of the Charles University

Supervisor: RNDr. Michal Pavelka, Ph.D., Mathematical Institute of the Charles University

Abstract: Rolling turbine is a small hydraulic turbine invented by Doc. Ing. Miroslav Sedláček CSc. in 1998. This turbine is bladeless, exhibits various interesting behaviour and operates on the basis of a yet unknown hydraulic principle. This thesis attempts to find an explanation using incompressible Navier-Stokes equations. We will introduce the concept of drag inversion - the idea that fluid force in rolling turbines is a positive feedback to the motion itself. This is explained in a simplified model using analytical methods. These results are then verified in a numerical simulation.

Keywords: rolling fluid turbine, fluid mechanics, stability, simulation

Contents

1 Introduction

A rolling turbine, also called a precession turbine or SETUR (SEdláček's TURbine) is a low-head water turbine invented by Czech engineer Miloš Sedláček in 1998 and is utilized to generate electricity on small rivers and streams. Main advantages of this design are (see [1], [4], [15]):

- Simplicity of construction and low maintenance costs.
- Reasonable efficiencies in range of 43-48% even for hydraulic heads bellow 1.6 m and flow rates below 3 l/s.
- The turbine is environment friendly and can be used in ecologically protected areas.

The turbine consist of an axially symmetric rotor inside a conical duct (the stator) to which it is connected by a shaft that is allowed to swivel freely around it's anchor point. When the rolling turbine runs, the rotor performs both rotary and precession movement — the latter is then used as a source of mechanical power which can be easily converted to electricity. Interestingly, the rotor has completely smooth shape[1] and does not have any blades, propellers or buckets. The hydraulic principle that powers this turbine is still unknown and is a subject of an ongoing scientific research, which currently lags behind experiments and applications. Simply put, it is known that SETUR is a functional design, but little is known about why. Naturally, this is a major obstacle in attempts to perfect this turbine.
This thesis attempts to resolve this problem. Although the dynamics of rolling turbines seems to be complex and non-linear, we suggest that basic understanding can be achieved relatively easily and using mostly linear theory. In developing our hypothesis, we aimed to explain numerous peculiar properties of SETUR obtained in the experiments. These are[2]:

1. Initially, the rotor and the stator are in a concentric configuration. When the water flows, the rotor will stick to the wall by itself. (Note that the rotor can be suspended from above and the rotor is heavier than water so this motion can occur against the force of gravity.)
2. If the rolling turbine has an axially symmetric design, then the direction of the precession is essentially random, meaning that it likely depends only on small imperfections and initial perturbations.

[1] Commonly used shapes are spheres, cones, hemispheres and disks.
[2] This list is based on our correspondence with Miloš Sedláček and on [1].

3. The water can be ducted tangentially, such that a vortex is generated at the inflow. **Even in this case, the turbine can precede both in the direction of the vortex or against it**. However, obtained power is somewhat smaller in the second case. The direction of precession can be swapped manually on the run — a brief mechanical impulse is sufficient.

4. When the rotor's swivel is obstructed in one direction, the rotor begins to vibrate erratically instead.

5. Thin gap between the rotor and the stator is a vital part of the design. Also, the rotor must have a convergent geometry, such that it's cross sectional area decreases in the direction of flow.

6. When the precession is performed manually, the turbine can operate as a water pump.

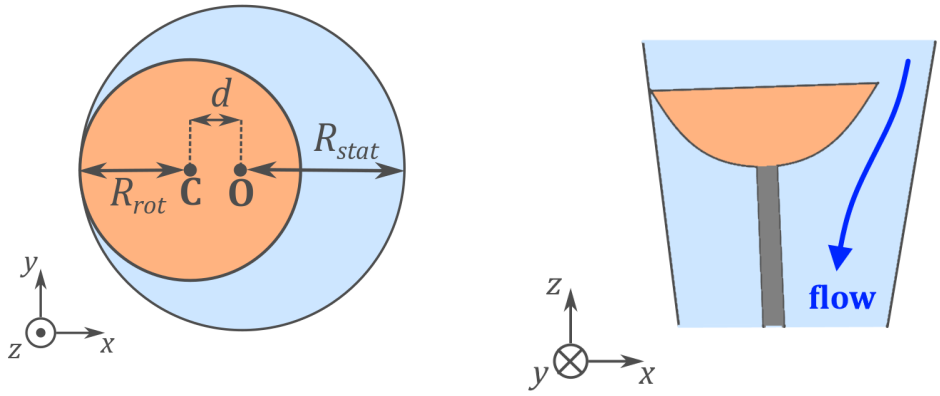

(a) top view

(b) side view

Figure 1: Schematic representation of a hemispherical rolling turbine.

Section 2 contains only standard theory and can be skipped freely. The section 3 is an analysis of the quiescent concentric configuration. This section is a recalculation of the paper [3]. The most important section is 4. There, we will introduce the idea of *drag inversion* and we will try to explain it in a special setting, where the turbine is already rolling steadily. We will see, that it is consistent with the property 3 above. Generalizing this to non-orbital motion and simplifying, we obtain an ODE system for the rotor and we will show that it is in accordance with properties 1,2 and 4. Finally, in 5, we will put these ideas into test using numerical methods. This will also allow us to take into account the geometry without simplifications,

which shows consistency with property 5. What is still unclear to the author is the relation between the motion of the rotor and the gradient of pressure needed for turbine performance. This is also related to property 6. Regarding this question, more research will be needed.

2 Fluid mechanics: preliminaries

The purpose of this chapter is to recall some central concepts of fluid mechanics (Navier-Stokes, Euler's equations, etc.) and to make the reader familiar with our notation. Only brief motivations are provided - for more detailed discussion see [2].

2.1 Cauchy momentum equations

Let U denote a volume occupied by a fluid. In general (and this is indeed the case for a turbine) the domain U may vary with time, i.e. $U = U(t)$ for t in some interval I (the time span of interest). We shall assume that U is an open and connected domain for all times t and is changing with time in a continuous manner, meaning that for every t_0 in I and every x_0 in $U(t_0)$ we can find $\delta > 0$ and an open ball B around x_0 such that $B \subset U(t)$ for all $t \in (t_0 - \delta, t_0 + \delta)$. The total space-time domain will be denoted by

$$\mathcal{U} = \{(\boldsymbol{x}, t) \in U(t),\, t \in I\} \tag{1}$$

To derive the equations, the first thing we consider is the conservation of mass: Let $x_0 \in U(t_0)$ and find B as above. We postulate that the change of mass inside the volume B must equate the amount of flux trough its boundary (meaning that no mass is being "lost"). This can be expressed integral-wise as

$$\frac{\mathrm{d}}{\mathrm{d}t} \int_B \rho \, \mathrm{d}\boldsymbol{x} = - \int_{\partial B} \rho \boldsymbol{u} \cdot \boldsymbol{n} \, \mathrm{d}S, \tag{2}$$

where $\rho \in C^1(\mathcal{U})$ is density of the fluid, $\boldsymbol{u} \in C^2(\mathcal{U}, \mathbb{R}^3)$ is the Eulerian velocity field and $\boldsymbol{n}$ is the outward normal. On the left, we can swap the order of integration and time-derivation. The right hand side can be turned into a volume integral using the Green's formula. This yields

$$\int_B \left[\frac{\partial \rho}{\partial t} + \operatorname{div}(\rho \boldsymbol{u}) \right] \, \mathrm{d}\boldsymbol{x} = 0. \tag{3}$$

Now, this must hold for arbitrary choice of x_0 and arbitrarily small B. Since the integrand is continuous, this is only possible if

$$\frac{\partial \rho}{\partial t} + \operatorname{div}(\rho \boldsymbol{u}) = 0 \tag{4}$$

point-wise for any $(\boldsymbol{x}, t) \in \mathcal{U}$. This result is known as the *continuity equation*. Some fluids, like water, are extremely difficult to compress and then we may suppose that

the density ρ is constant throughout space and time. This allows us to simplify and write

$$\operatorname{div} \boldsymbol{u} = 0. \tag{5}$$

Secondly, we consider the Newton's second law. In this setting, it tells us that the change of momentum inside B is equal to the flux of momentum through boundary plus the total amount of volume forces $\boldsymbol{f} \in C(\mathcal{U}, \mathbb{R}^3)$ (such as gravitation) and the surface forces (such as pressure) given by stress tensor $\mathbb{T} \in C^1(\mathcal{U}, \mathbb{R}^{3\times 3})$. Mathematically, this gives the following

$$\frac{\mathrm{d}}{\mathrm{d}t} \int_B \rho \boldsymbol{u} \, \mathrm{d}\boldsymbol{x} = - \int_{\partial B} \rho \left(\boldsymbol{u} \otimes \boldsymbol{u}\right) \boldsymbol{n} \, \mathrm{d}S + \int_B \rho \boldsymbol{f} \, \mathrm{d}\boldsymbol{x} + \int_{\partial B} \mathbb{T} \boldsymbol{n} \, \mathrm{d}S. \tag{6}$$

Again, by using Green's theorem and deriving after the integration sign we can turn this equation into one volume integral over B:

$$\int_B \left\{ \frac{\partial \left(\rho \boldsymbol{u}\right)}{\partial t} + \operatorname{div} \left[\rho \left(\boldsymbol{u} \otimes \boldsymbol{u}\right)\right] - \rho \boldsymbol{f} - \operatorname{div} \mathbb{T} \right\} \, \mathrm{d}\boldsymbol{x} = 0. \tag{7}$$

As before, this can be satisfied for every B only when

$$\frac{\partial \left(\rho \boldsymbol{u}\right)}{\partial t} + \operatorname{div} \left[\rho \left(\boldsymbol{u} \otimes \boldsymbol{u}\right)\right] = \rho \boldsymbol{f} + \operatorname{div} \mathbb{T}. \tag{8}$$

Using the continuity equation (4), we have

$$\begin{aligned} \frac{\partial \left(\rho \boldsymbol{u}\right)}{\partial t} + \operatorname{div} \left[\rho \left(\boldsymbol{u} \otimes \boldsymbol{u}\right)\right] &= \frac{\partial \rho}{\partial t} \boldsymbol{u} + \rho \frac{\partial \boldsymbol{u}}{\partial t} + \operatorname{div} \left(\rho \operatorname{div} \boldsymbol{u}\right) \boldsymbol{u} + \rho \left(\left(\nabla \cdot \boldsymbol{u}\right) \boldsymbol{u}\right) \\ &= \rho \left[\frac{\partial \boldsymbol{u}}{\partial t} + \left(\nabla \cdot \boldsymbol{u}\right) \boldsymbol{u} \right] \end{aligned} \tag{9}$$

By plugging this into (8) we obtain the *Cauchy momentum equations*:

$$\frac{\partial \boldsymbol{u}}{\partial t} + \left(\nabla \cdot \boldsymbol{u}\right) \boldsymbol{u} = \boldsymbol{f} + \frac{1}{\rho} \operatorname{div} \mathbb{T}. \tag{10}$$

2.2 Navier-Stokes equations

The description of a fluid is not complete until one specifies the stress tensor $\mathbb{T}$. For an incompressible *Newtonian fluid*, it is given by formula:

$$\mathbb{T} = -p\mathbb{I} + 2\rho\nu\mathbb{D}, \tag{11}$$

where $p \in C^1(\mathcal{U})$ is pressure and the second term represents viscous forces: constant ν is the kinematic viscosity coefficient and

$$\mathbb{D} = \frac{1}{2}\left(\nabla \boldsymbol{u} + \nabla \boldsymbol{u}^T\right). \tag{12}$$

Using incompressibility ($\operatorname{div} \boldsymbol{u} = 0$) we calculate

$$\hat{\boldsymbol{e}}_i \cdot \operatorname{div} \mathbb{T} = \frac{\partial\, \mathbb{T}_{ij}}{\partial\, \boldsymbol{x}_j} = \frac{\partial}{\partial\, \boldsymbol{x}_j}\left(-p\delta_{ij} + \rho\nu \frac{\partial\, \boldsymbol{u}_i}{\partial\, \boldsymbol{x}_j} + \rho\nu \frac{\partial\, \boldsymbol{u}_j}{\partial\, \boldsymbol{x}_i}\right) = -p\frac{\partial\, p}{\partial\, \boldsymbol{x}_i} + \rho\nu \frac{\partial^2 \boldsymbol{u}_i}{\partial\, \boldsymbol{x}_j \boldsymbol{x}_j}, \tag{13}$$

which gives

$$\operatorname{div} \mathbb{T} = -\nabla p + \rho\nu \Delta \boldsymbol{u}. \tag{14}$$

Plugging this into (10) gives us the *incompressible Navier-Stokes equations*:

$$\frac{\partial\, \boldsymbol{u}}{\partial\, t} + (\nabla \cdot \boldsymbol{u})\, \boldsymbol{u} = \boldsymbol{f} - \frac{1}{\rho}\nabla p + \nu \Delta \boldsymbol{u}. \tag{15}$$

Together with the condition of incompressibility, they form a system of four partial differential equations with four unknowns: the three components of velocity field $\boldsymbol{u}$ and the pressure field p. The volume force $\boldsymbol{f}$, density ρ and kinematic viscosity ν must be prescribed.

2.3 Some thermodynamic aspects

In addition to the continuity and momentum equation, it is also possible to derive[3] the evolutionary equation for the specific entropy s, which reads:

$$\rho\left(\frac{\partial\, s}{\partial\, t} + (\nabla \cdot \boldsymbol{u})\, s\right) + \operatorname{div} \boldsymbol{j}_{\boldsymbol{\eta}} = \frac{\xi_\eta}{\tau},$$

where τ is temperature, j_η is the entropy flux and

$$\xi = \mathbb{T} : \mathbb{D} = 2\rho\nu \mathbb{D} : \mathbb{D}$$

is the dissipation[4]. We will not need this equation it's full scope. We would only like the mention the principle of *minimal entropy production*, which asserts that close to equilibrium, systems evolve towards a state where entropy production is small. In case of Navier Stokes equations, due to the presence of a convective term,

[3] see [2] or [9]

[4] This expresses the amount of mechanical energy in fluid that is transformed into heat. Positivity of this term makes the Navier-Stokes equations compatible with the second law of thermodynamics.

this principle does not strictly hold — it is merely a general observation that when a system evolves from one state to another, the dissipation in the fluid typically increases initially, only to fall down in the end. It can be therefore interesting to plot ξ in a numerical computation as it helps to infer whether the fluid is going to reach an equilibrium any time soon. For more on this matter, see [9].

2.4 Forces acting on an immersed rigid body

Once a solution to a problem is obtained (be it analytical or numerical), a common question is what are the fluid forces on some body of interest (e.g. the rotor). For an incompressible Navier-Stokes (15), the surface density of force which acts on an immersed rigid body R is given by:

$$\boldsymbol{G} = -\mathbb{T}\boldsymbol{n} \tag{16}$$

where $\boldsymbol{n}$ is the outer normal vector to its surface ∂R. Using the formula (14), the vector $\boldsymbol{G}$ may be decomposed into a pressure component $\boldsymbol{G}_p = p\boldsymbol{n}$, which is always orthogonal to the surface, and a viscous part $\boldsymbol{G}_v = -2\rho\nu\mathbb{D}\boldsymbol{n}$, which (slightly less trivially) always points tangentially to the surface. In order to see this, consider arbitrary $\boldsymbol{x}_0 \in \partial R$ and a local parametrization [5] $\boldsymbol{x} = \boldsymbol{\varphi}(\sigma, \tau)$ of ∂R. Then, we may define the following tangent vectors:

$$\boldsymbol{t}_\sigma = \frac{\partial \varphi}{\partial \sigma}, \quad \boldsymbol{t}_\tau = \frac{\partial \varphi}{\partial \tau}. \tag{17}$$

Without loss of generality, we may assume that $\boldsymbol{t}_\sigma, \boldsymbol{t}_\tau$ are orthonormal [6] at x_0. The motion of a rigid body can be described entirely by the velocity $\boldsymbol{u}_0$ of its centre of mass $\boldsymbol{x}_T$ and the angular velocity $\boldsymbol{\Omega}$. This yields a no-slip boundary condition for the fluid

$$\boldsymbol{u} = \boldsymbol{u}_0 + \boldsymbol{\Omega} \times (\boldsymbol{x} - \boldsymbol{x}_T), \qquad \boldsymbol{x} \in \partial R. \tag{18}$$

Letting $\boldsymbol{x} = \boldsymbol{\varphi}(\sigma, \tau)$ and differentiating with respect to σ at $\boldsymbol{x}_0$ gives

$$\nabla \boldsymbol{u}\, \boldsymbol{t}_\sigma = \boldsymbol{\Omega} \times \boldsymbol{t}_\sigma. \tag{19}$$

Taking the dot product with $\boldsymbol{t}_\sigma$ on both sides then yields

$$\boldsymbol{t}_\sigma \cdot \mathbb{D}\, \boldsymbol{t}_\sigma = 0. \tag{20}$$

The same holds for $\boldsymbol{t}_\tau$. Finally, we use the invariance of trace with respect to change of basis to get

$$0 = \operatorname{div} \boldsymbol{u} = \operatorname{Tr} \mathbb{D} = (\boldsymbol{n} \cdot \mathbb{D}\, \boldsymbol{n}) + (\boldsymbol{t}_\sigma \cdot \mathbb{D}\, \boldsymbol{t}_\sigma) + (\boldsymbol{t}_\tau \cdot \mathbb{D}\, \boldsymbol{t}_\tau) = -\frac{1}{2\rho\nu} \boldsymbol{n} \cdot \boldsymbol{G}_v. \tag{21}$$

Thus $\boldsymbol{G}_v$ must lie in the tangent space of ∂R at every point $\boldsymbol{x}_0 \in \partial R$.

[5] Which we assume here to be $C^1(V)$ for some open subset V of $\mathbb{R}^2$.

[6] For if not, one can define $\hat{\varphi} = \varphi \circ a$ where a is an affine mapping, such that it holds for $\hat{\varphi}$.

2.5 Euler's equations and potential flow

It often happens in (15) that the viscosity term $\nu\Delta\boldsymbol{u}$ is very small. In such a case it makes sense to simplify by setting $\nu = 0$, which leads to the Euler's equations:

$$\frac{\partial\,\boldsymbol{u}}{\partial\,t} + (\nabla\cdot\boldsymbol{u})\,\boldsymbol{u} = \boldsymbol{f} - \frac{1}{\rho}\nabla p. \tag{22}$$

A problem occurs because we are effectively omitting the term with highest (i.e. second) spatial partial derivative. This corresponds to the fact that for low ν, near solid surfaces, there is typically a region where $\boldsymbol{u}$ steeply rises from zero and where the viscous term dominates in spite of small ν (the so called *boundary layer*). This issue can be circumvented somewhat by assuming that the boundary layer is so thin that it can be neglected and the fluid is allowed to slip on a surface.

In the case where the volume force is conservative, i.e. there exists a potential ψ such that $\boldsymbol{f} = -\nabla\psi$, the famous *Kelvin's theorem* applies. It tells us that for any time-dependant curve $\gamma = \gamma(s,t) \in U(t)$ of the class $C^1([0,1]\times I, \mathbb{R}^3)$ which satisfies

$$\frac{\partial\,\gamma}{\partial\,t}(s,t) = \boldsymbol{u}(\gamma(s,t),t) \tag{23}$$

(i.e. γ is a material curve - for all t it is composed of the same "fluid particles") it holds that the amount of circulation through γ is constant

$$\frac{\mathrm{d}}{\mathrm{d}t}\int_{\gamma(\cdot,t)} \boldsymbol{u}\cdot\,\mathrm{d}\gamma(s) = 0. \tag{24}$$

Hence, if we imagine that the fluid is initially in a state with no circulation (such as being at rest), then by (24) we observe that the circulation will remain always zero [7]. Under these assumptions, there exists [8] a potential φ, such that

$$\boldsymbol{u} = \nabla\varphi. \tag{25}$$

We then say that $\boldsymbol{u}$ is a potential flow and as such it automatically satisfies $\operatorname{rot}\boldsymbol{u} = 0$. Using the identity

$$(\nabla\cdot\boldsymbol{u})\,\boldsymbol{u} = \nabla\left(\frac{u^2}{2}\right) + (\operatorname{rot}\boldsymbol{u})\times\boldsymbol{u}, \tag{26}$$

and $\boldsymbol{f} = -\nabla\psi$ we can rewrite equation (22) as

$$\frac{\partial}{\partial\,t}(\nabla\varphi) + \nabla\left(\frac{u^2}{2}\right) = -\nabla\psi - \frac{1}{\rho}\nabla p \tag{27}$$

[7] Of course, when ν is not exactly zero then circulation may build up slowly over time.

[8] Follows from the fundamental field theorem [2]; notice that this implication doesn't require $U(t)$ to be simply connected.

$$\nabla\left(\frac{\partial\varphi}{\partial t}+\frac{u^2}{2}+\psi+\frac{p}{\rho}\right)=0. \tag{28}$$

Using that $U(t)$ is connected, this is possible only when

$$\frac{\partial\varphi}{\partial t}+\frac{u^2}{2}+\psi+\frac{p}{\rho}=b. \tag{29}$$

where $b=b(t)$ is a function independent of the space variable $\boldsymbol{x}$. This is the famous *Bernoulli's equation*. What remains then, is to solve for φ using the condition of incompressibility $\operatorname{div}\boldsymbol{u}=0$ which leads to the *Laplace equation*:

$$\Delta\varphi=0. \tag{30}$$

3 Laminar Breakdown in a Divergent Channel

The work of J. Falta and F. Maršík [3] focuses on studying the initial configuration of the rotor which exists briefly before the turbine begins to operate. Following their interesting paper, we analyse here the problem of incompressible viscous flow in a channel between a cylinder and a coaxial truncated cone. The geometry can be described in cylindrical coordinates as follows:

$$U = \left\{(r, \theta, z): \quad R_{\text{rot}} + \gamma z < r < R_{\text{stat}}; \quad z \in (-L, 0)\right\},$$

where R_{stat} denotes the diameter of the outer cylinder (the stator), R_{rot} is the maximal radius of the inner cone (the rotor) and

$$\arctan \gamma$$

is its half-apex angle. Now, we imagine that a stream of water flows through U such that it enters at $z = 0$ and exits at $z = -L$. Considering the symmetry of the problem, it makes sense to assume for the velocity field and pressure:

$$\boldsymbol{u} = \begin{pmatrix} u_r(r, z) \\ 0 \\ u_z(r, z) \end{pmatrix}, \quad p = p(r, z). \tag{31}$$

According to Maršík [1], however, such a symmetry is inherently unstable and imperfections — no matter how small — give rise to strong asymmetric volume forces. The instability of the initial configuration is suspected to be a manifestation of this phenomenon.

To make things easier, we find an approximate formula for velocity field using the assumption (31) and observe the situation where the inflow is large. We begin be writing the stationary Navier-Stokes equations (15) in cylindrical coordinates:

$$\begin{aligned}
(\nabla \cdot \boldsymbol{u})\, u_r + \frac{u_\theta^2}{r} &= -\frac{1}{\rho}\frac{\partial p}{\partial r} + \nu\left\{\Delta u_r - \frac{2}{r^2}\frac{\partial u_\theta}{\partial \theta} - \frac{u_r}{r^2}\right\} \\
(\nabla \cdot \boldsymbol{u})\, u_\theta + \frac{u_r u_\theta}{r} &= -\frac{1}{\rho r}\frac{\partial p}{\partial \theta} + \nu\left\{\Delta u_\theta + \frac{2}{r^2}\frac{\partial u_r}{\partial \theta} - \frac{u_\theta}{r^2}\right\} \\
(\nabla \cdot \boldsymbol{u})\, u_z &= -\frac{1}{\rho}\frac{\partial p}{\partial z} + \nu \Delta u_z
\end{aligned} \tag{32}$$

together with the equation of continuity:

$$\frac{\partial u_r}{\partial r} + \frac{1}{r}\frac{\partial u_\theta}{\partial \theta} + \frac{\partial u_z}{\partial z} + \frac{u_r}{r} = 0. \tag{33}$$

With (31), the second equation in (32) is solved trivially and our problem is then effectively reduced to a system of three equations with three unknowns: u_r, u_z, p. The next step is to reformulate the system using dimensionless variables. This allows us to compare orders of magnitude among terms appearing in the equations. To this end, we introduce the characteristic velocity U_{char} and the characteristic length L_{char} as

$$U_{\text{char}} = \max_{(r,z)} |u_z|, \quad L_{\text{char}} = R_{\text{stat}},$$

which allow us to define the dimensionless coordinates and velocity by

$$\hat{\boldsymbol{u}} = \frac{\boldsymbol{u}}{U_{\text{char}}}, \quad \hat{r} = \frac{r}{L_{\text{char}}}, \quad \hat{z} = \frac{z}{L_{\text{char}}}.$$

Now, multiplying (32) by $L_{\text{char}}/U_{\text{char}}^2$ and (33) by $L_{\text{char}}/U_{\text{char}}$ and employing the symmetry (31) yields the following dimensionless system [9]:

$$\begin{aligned} \left(\hat{\boldsymbol{u}} \cdot \hat{\nabla}\right) \hat{u}_r &= -\frac{\partial \hat{p}}{\partial \hat{r}} + \frac{1}{\text{Re}} \left\{ \hat{\Delta} \hat{u}_r - \frac{\hat{u}_r}{\hat{r}^2} \right\} \\ \left(\hat{\boldsymbol{u}} \cdot \hat{\nabla}\right) \hat{u}_z &= -\frac{\partial \hat{p}}{\partial \hat{z}} + \frac{1}{\text{Re}} \hat{\Delta} \hat{u}_z \end{aligned} \tag{34}$$

and

$$\frac{\partial \hat{u}_r}{\partial \hat{r}} + \frac{\partial \hat{u}_z}{\partial \hat{z}} + \frac{\hat{u}_r}{\hat{r}} = 0. \tag{35}$$

Here, the dimensionless pressure $\hat{p}$ is defined as

$$\hat{p} = \frac{p}{\rho U_{\text{char}}^2}$$

and

$$\text{Re} = \frac{L_{\text{char}} U_{\text{char}}}{\nu}$$

is the corresponding *Reynolds number*. The next trick is to make a transformation of coordinates [10]

$$\begin{aligned} \xi &= 1 - \frac{1 - \hat{r}}{b}, \\ \zeta &= \hat{z}, \end{aligned}$$

where

$$b(\hat{z}) = \frac{1}{2} \left(1 - \gamma \hat{z} - \frac{R_{\text{rot}}}{R_{\text{stat}}} \right)$$

[9] Hat above an operator signifies differentiation with respect to dimensionless coordinates $\hat{r}$, $\hat{z}$.

[10] Here it is useful to rename the $\hat{z}$ variable so that $\partial/\partial\zeta$ denotes the partial derivative where ξ and not $\hat{r}$ is being fixed.

is — up to a normalization factor — the size of gap between the stator and the rotor at height $\hat{z}$. Thus, ξ is an affine transformation of $\hat{r}$ such that the surface of the inner cone corresponds to $\xi = -1$ and the surface of the outer cylinder corresponds to $\xi = 1$. The partial derivatives are then related through the transposed Jacobi matrix as follows:

$$\begin{pmatrix} \frac{\partial}{\partial \hat{r}} \\ \frac{\partial}{\partial \hat{z}} \end{pmatrix} = \begin{pmatrix} \frac{1}{b} & 0 \\ -\frac{\gamma}{2b}(1-\xi) & 1 \end{pmatrix} \begin{pmatrix} \frac{\partial}{\partial \xi} \\ \frac{\partial}{\partial \zeta} \end{pmatrix}.$$

Before we substitute this into (34) and (35), let us make the following assumptions on the orders of magnitude:

$$\begin{aligned} b_0 := b(0) &\ll 1, \\ \gamma, b, \hat{u}_r, \nabla_{\xi,\zeta}\hat{u}_r, \nabla^2_{\xi,\zeta}\hat{u}_r &= O(b_0), \\ \hat{u}_z, \nabla_{\xi,\zeta}\hat{u}_z, \nabla^2_{\xi,\zeta}\hat{u}_z &= O(1), \\ \frac{1}{\mathrm{Re}} &= O(b_0^2) \end{aligned}$$

That is, we assume the gap between the cylinder and the rotor to be very thin and the inner cone to be relatively narrow. Correspondingly, the flow velocity field will be dominated by the $\hat{u}_z$ component, $\hat{u}_r$ being small. This is also assumed for all the first and second derivatives with respect to ξ, ζ. Lastly, the viscous forces in the fluid are assumed to be weak. With this, we get the following approximation of the Laplace operator for $\varphi = \hat{u}_r, \hat{u}_z$:

$$\hat{\Delta}\varphi = \frac{1}{b^2}\left(\frac{\partial^2 \varphi}{\partial \xi^2} + O(b_0)\right)$$

an the first equation in (34) then yields

$$\frac{\partial \hat{p}}{\partial \xi} = b\frac{\partial \hat{p}}{\partial \hat{r}} = -b\left(\hat{\boldsymbol{u}} \cdot \hat{\nabla}\right)\hat{u}_r + \frac{b}{\mathrm{Re}}\left(\hat{\Delta}\hat{u}_r - \frac{\hat{u}_r}{\hat{r}^2}\right) = O(b_0), \tag{36}$$

from the second equation it follows that

$$\begin{aligned} \left(\hat{\boldsymbol{u}} \cdot \hat{\nabla}\right)\hat{u}_z &= +\frac{\gamma}{2b}(1-\xi)\frac{\partial \hat{p}}{\partial \xi} - \frac{\partial \hat{p}}{\partial \zeta} + \frac{1}{\mathrm{Re}}\hat{\Delta}\hat{u}_z \\ &= -\frac{\partial \hat{p}}{\partial \zeta} + \frac{1}{b^2 \mathrm{Re}}\frac{\partial^2 u_z}{\partial \xi^2} + O(b_0) \end{aligned} \tag{37}$$

and the continuity equation (35) becomes

$$\frac{1}{b}\frac{\partial \hat{u}_r}{\partial \xi} - \frac{\gamma}{2b}(1-\xi)\frac{\partial \hat{u}_z}{\partial \xi} + \frac{\partial \hat{u}_z}{\partial \zeta} + \frac{\hat{u}_r}{\hat{r}} = 0,$$

which gives (after some manipulations)

$$\frac{\partial}{\partial \xi}\left[\hat{u}_r - \frac{\gamma}{2}(1-\xi)\hat{u}_z\right] + \frac{\partial}{\partial \zeta}(b\hat{u}_z) = O(b_0). \tag{38}$$

An approximate equation is then deduced from (36), (37), (38) by neglecting all terms of order $O(b_0)$.

$$\begin{aligned} \frac{\partial \hat{p}}{\partial \xi} &= 0, \\ \left(\hat{\boldsymbol{u}} \cdot \hat{\nabla}\right) \hat{u}_z &= -\frac{\partial \hat{p}}{\partial \zeta} + \frac{1}{b^2 \mathrm{Re}} \frac{\partial^2 u_z}{\partial \xi^2} \end{aligned} \tag{39}$$

and

$$\frac{\partial}{\partial \xi}\left[\hat{u}_r - \frac{\gamma}{2}(1-\xi)\hat{u}_z\right] + \frac{\partial}{\partial \zeta}(b\hat{u}_z) = 0. \tag{40}$$

This system can be solved easily by the ansatz

$$\begin{aligned} b\hat{u}_z &= -b_0 q, \\ \hat{u}_r &= \frac{\gamma}{2}(1-\xi)\hat{u}_z, \end{aligned} \tag{41}$$

where $q = q(\xi)$ is (yet unknown) function of ξ. This satisfies (40) trivially and greatly simplifies the convective term

$$\begin{aligned} \left(\hat{\boldsymbol{u}} \cdot \hat{\nabla}\right) \hat{u}_z &= \frac{\partial \hat{u}_z}{\partial \hat{z}} \hat{u}_r + \frac{\partial \hat{u}_z}{\partial \hat{r}} \hat{u}_z \\ &= \frac{1}{b} \frac{\partial \hat{u}_z}{\partial \xi} \hat{u}_r - \frac{\gamma}{2b}(1-\xi) \frac{\partial \hat{u}_z}{\partial \xi} \hat{u}_z + \frac{\partial \hat{u}_z}{\partial \zeta} \hat{u}_z. \\ &= \frac{\partial \hat{u}_z}{\partial \zeta} \hat{u}_z \end{aligned}$$

By plugging it into (39) we obtain

$$q'' + \frac{1}{2}\gamma b_0 \, \mathrm{Re} \, q^2 = -\frac{b^3 \mathrm{Re}}{b_0} \frac{\partial \hat{p}}{\partial \zeta}.$$

Differentiating both sides with respect to ξ and defining

$$\mathrm{Re}^* = \gamma b_0 \mathrm{Re}$$

yields an ordinary differential equation of the third order [11] for q:

$$q''' + \mathrm{Re}^* q q' = 0. \tag{42}$$

[11] which is, not surprisingly, similar to the situation in Jeffery-Hamell flow

We are naturally interested in a solution which complies with the following conditions:

$$\begin{aligned} q(\xi) \in (0,1]\,, &\quad \xi \in [-1,1]\,, \\ q(\xi) = 0, &\quad \xi = \pm 1, \\ \exists \xi_0 \in (-1,1): &\quad q(\xi_0) = 1. \end{aligned} \tag{43}$$

This fixes downward direction of the flow, ensures no slip at the edges and sets the maximal value to $q = 1$ (corresponding to the choice of U_{char}). Then necessarily $q'(\xi_0) = 0$ and from (42) it is easy to see that q is even around ξ_0. So it must be that $\xi_0 = 0$. Let us integrate the equation back, to get

$$q'' + \frac{1}{2}\mathrm{Re}^* q^2 = C, \tag{44}$$

for some integration constant C. Multiplying both sides by q', we can integrate once more to find

$$\frac{1}{2}(q')^2 = -C(1-q) + \frac{1}{6}\mathrm{Re}^*(1-q^3), \tag{45}$$

where the second integration constant had to be fixed such that $q' = 0$ for the maximal value $q = 1$. Redefining the first integration constant as

$$C^* = 1 - \frac{6C}{\mathrm{Re}^*}$$

and doing some algebra, the equation (45) can be written in a nicer form

$$(q')^2 = \frac{\mathrm{Re}^*}{3}(1-q)(C^* + q + q^2).$$

It surely must be that $C^* \geq 0$, for else we would have $(q')^2 < 0$ at $\xi = \pm 1$. By separating the variables, we get

$$I(C^*) := \int_0^1 \frac{\mathrm{d}q}{\sqrt{(1-q)(C^* + q + q^2)}} = \int_{-1}^0 \sqrt{\frac{\mathrm{Re}^*}{3}}\,\mathrm{d}\xi = \sqrt{\frac{\mathrm{Re}^*}{3}}. \tag{46}$$

Note that the integral converges for any value of $C^* \geq 0$ and is a strictly decreasing function of C^*. Thus, for any value of Re^* at most one solution satisfying (43) exists: it is the solution of (44) with the initial condition

$$q(-1) = 0 \qquad q'(-1) = \sqrt{\frac{\mathrm{Re}^* C^*}{3}},$$

where C^* is uniquely fixed by (46). Not for every value of $\mathrm{Re}^* > 0$ is there a solution, however, since the integral $I(C^*)$ can only attain values from

$$\lim_{C^*\to\infty} I(C^*) = 0$$

to its maximal value

$$\begin{aligned} I(0) &= \int_0^1 \frac{\mathrm{d}q}{\sqrt{q(1-q^2)}} = \left| \begin{array}{c} s = q^2 \\ \mathrm{d}s = 2\sqrt{s}\,\mathrm{d}q \end{array} \right| = \frac{1}{2}\int_0^1 s^{-3/4}(1-s)^{-1/2}\,\mathrm{d}s \\ &= \frac{1}{2}B\left(\frac{1}{4},\,\frac{1}{2}\right) = \frac{\sqrt{\pi}\,\Gamma(\frac{1}{4})}{2\Gamma(\frac{3}{4})}. \end{aligned}$$

This, in light of (46), leads to a certain critical Reynolds number

$$\mathrm{Re}^*_{\mathrm{crit}} = \frac{3}{4}\pi\left(\frac{\Gamma(\frac{1}{4})}{\Gamma(\frac{3}{4})}\right)^2 \approx 20.62.$$

Above this value, solutions satisfying (43) may no longer exist. One can only lift the assumption of $q \geq 0$ to get non-unique velocity profiles with back-flows. The paper [3] then proceeds with stability analysis, but it relies on some assumptions that we were not able to understand. Also it seems to us, that stability analysis alone — while certainly insightful — is more of a negative result: it indicates that something should occur but does not exactly explain what should happen and why. Motivated by belief that simple explanation of the hydraulic principle should be possible, we shall present our own and different approach in the following sections.

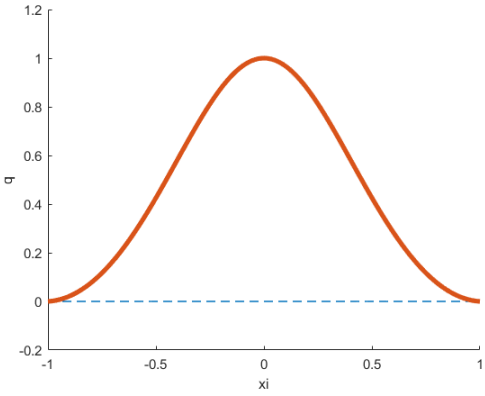

(a) $\mathrm{Re}^* = 20$

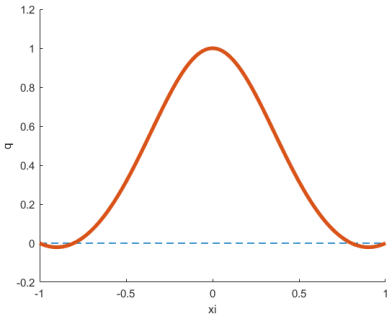

(b) $\mathrm{Re}^* = 26$

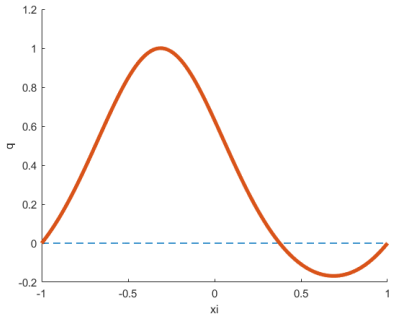

(c) $\mathrm{Re}^* = 26$

Figure 2: Numerically computed q for different values of Re^*. For high Re^*, the solutions are non-unique.

4 Analysis of the Hydraulic Principle

In this section, we will describe our understanding of SETUR by means of analytical methods. The underlying idea is that the pressure field, which propels the turbine, exists as a reaction to the rotor's motion. When the flow through turbine is zero, any motion of the turbine will be opposed by friction in accordance with the second law of thermodynamics. The situation may become different in the presence of flow, where, due to the energy of the flow, the drag force will switch the sign — the water will react to orbital motion by accelerating it — this is what we call *drag inversion*. We will try to unveil this strange behaviour by analysing temporal variations in fluid velocity. To avoid a time-dependant problem with variable geometry, we shall switch to what we call *co-precessing frame of reference*, where we will assume that the problem is stationary. Our approach is following: We prescribe boundary conditions assuming that the rotor is rolling steadily. Then, we will try to obtain some information about pressure field. Finally, switching back to the inertial frame, power on the rotor can be computed. If this power is positive, it means that it can be extracted from the system, as otherwise, the rotor would accelerate. This approach will hopefully address two problems at once: firstly the question of instability and secondly, where does the power output of rolling turbine come from. Similar method can be used for numerical analysis, which we will do later in section (5).

4.1 Co-precessing frame of reference

Let us assume that the rotor is a truncated cone and that the stator is a cylinder with radius R_{stat}. In practise, the rotor would be suspended from above or bellow by a shaft and rotate around an inclined preceding axis. To simplify matters, however, we will assume that the axis is at all times parallel with the rotor as if the shaft was held on gears that move along with the rotor's rolling motion. We shall orient our axes so that $\hat{\boldsymbol{z}}$ is the stator's symmetry axis and so that the contact with rotor occurs at $z = 0$. Let $R_{\text{rot}}(z)$ denote the rotor's radius. We set the direction of $\hat{\boldsymbol{z}}$ so that $R_{\text{rot}}(z)$ is an increasing affine function of z. (Thus $z = 0$ is the "top" and our domain of interest is the diverging gap between the cone and the cylinder for $z < 0$). Let $\boldsymbol{C}$ be the point where rotor's symmetry axis intersects $z = 0$ (the centre of the topmost circular cross-section) and assume that the rate of turbine precession is Ω and is clockwise when viewed from above, i.e.:

$$\boldsymbol{u}_{\boldsymbol{C}} = \frac{\mathrm{d}\boldsymbol{C}}{\mathrm{d}t} = -\Omega\hat{\boldsymbol{z}} \times \boldsymbol{C}. \tag{47}$$

The rotor will then rotate around it's own symmetry axis counter-clockwise with angular velocity Ω_{rot}. Any point $\boldsymbol{x}$, which lies on the surface of the rotor, has

velocity

$$\boldsymbol{u} = \frac{\mathrm{d}\boldsymbol{x}}{\mathrm{d}t} = \boldsymbol{u_C} + \frac{\mathrm{d}}{\mathrm{d}t}\left(\boldsymbol{x} - \boldsymbol{C}\right) = -\Omega\hat{\boldsymbol{z}} \times \boldsymbol{C} + \Omega_{\mathrm{rot}}\hat{\boldsymbol{z}} \times \left(\boldsymbol{x} - \boldsymbol{C}\right). \tag{48}$$

The value of Ω_{rot} can be determined by assuming a no-slip contact between the stator and the rotor. Without loss of generality, we can assume that at time $t = 0$, we have $\boldsymbol{C} = (-d, 0, 0)^T$, where $d = R_{\mathrm{stat}} - R_{\mathrm{rot}}(0)$. Plugging this into (48), we get:

$$\boldsymbol{u}|_{t=0} = \begin{pmatrix} -\Omega_{\mathrm{rot}} y \\ \Omega d + \Omega_{\mathrm{rot}}(x + d) \\ 0 \end{pmatrix} \tag{49}$$

This velocity $\boldsymbol{u}$ has to be zero at $\boldsymbol{x} = (-R_{\mathrm{stat}}, 0, 0)^T$, which means that

$$\Omega_{\mathrm{rot}} = \frac{\Omega d}{R_{\mathrm{rot}}(0)} \tag{50}$$

and

$$\boldsymbol{u}|_{t=0} = \Omega_{\mathrm{rot}} \begin{pmatrix} -y \\ R_{\mathrm{stat}} + x \\ 0 \end{pmatrix}. \tag{51}$$

Now, it is interesting to determine the component velocity in the direction of the surface normal. Let

$$x + d = R_{\mathrm{rot}}(z)\cos\theta', \qquad y = R_{\mathrm{rot}}\sin\theta'. \tag{52}$$

(θ' is the angular coordinate as measured from C). This allows to rewrite (51) as

$$\boldsymbol{u}|_{t=0} = \Omega_{\mathrm{rot}} R_{\mathrm{rot}}(0) \begin{pmatrix} -\beta\sin\theta' \\ 1 + \beta\cos\theta' \\ 0 \end{pmatrix}, \tag{53}$$

where $\beta(z) = R_{\mathrm{rot}}(z)/R_{\mathrm{rot}}(0)$. Let us denote $\gamma = R'_{\mathrm{rot}} = \mathrm{const}$. Then, the rotor's surface normal at $(x, y, z)^T$ is

$$\boldsymbol{n} = \frac{1}{\sqrt{1 + \gamma^2}} \begin{pmatrix} \cos\theta' \\ \sin\theta' \\ -\gamma \end{pmatrix} \tag{54}$$

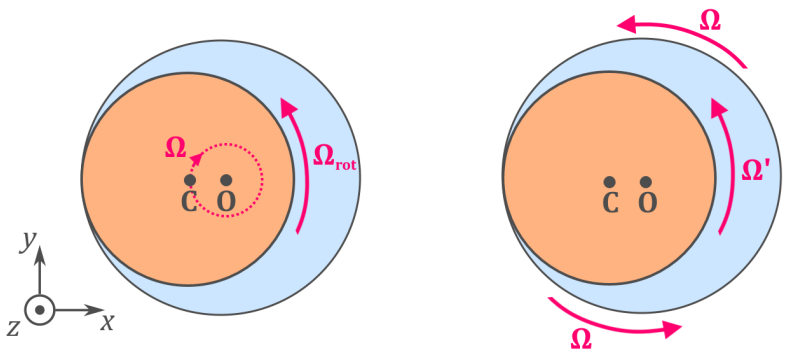

Figure 3: angular velocities in the inertial (left) and the co-precessing frame (right)

and the normal component $v_{\boldsymbol{n}}$ of velocity $\boldsymbol{u}$ at $t = 0$ can be computed as

$$v_{\boldsymbol{n}} = \boldsymbol{u}|_{t=0} \cdot \boldsymbol{n} = \frac{\Omega_{\text{rot}} R_{\text{rot}}(0)}{\sqrt{1+\gamma^2}} \sin\theta'. \tag{55}$$

This reveals a somewhat counter-intuitive fact, that for fixed Ω_{rot}, the amount of normal velocity of a rolling turbine does not depend on the size of gap $2d$ [12]. This is important, because the pressure force can generate power only through the normal component of velocity and for SETUR, d is typically very small.

In general, problems in fluid mechanics with variable geometry are difficult. It is the therefore a good idea to switch into a co-precessing frame connected to an observer that rotates clockwise with angular velocity Ω. The coordinate transformation between these two frames (those in the co-precessing frame are denoted with upper script) is given by:

$$\begin{aligned} \tilde{x} &= x\cos(\Omega t) - y\sin(\Omega t), \\ \tilde{y} &= x\sin(\Omega t) + y\cos(\Omega t), \\ \tilde{z} &= z. \end{aligned} \tag{56}$$

All velocities in the co-precessing frame $\tilde{\boldsymbol{u}}$ are related to the corresponding velocities $\boldsymbol{u}$ in the inertial frame by

$$\tilde{\boldsymbol{u}} = \boldsymbol{u} + \Omega\hat{\boldsymbol{z}} \times \tilde{\boldsymbol{x}}. \tag{57}$$

We now have $\tilde{\boldsymbol{u}}_{\boldsymbol{C}} = 0$ and for any point $\tilde{\boldsymbol{x}}$ on the rotor's surface:

$$\tilde{\boldsymbol{u}} = -\Omega\hat{\boldsymbol{z}} \times \boldsymbol{C} + \Omega_{\text{rot}}\hat{\boldsymbol{z}} \times (\tilde{\boldsymbol{x}} - \boldsymbol{C}) + \Omega\hat{\boldsymbol{z}} \times \tilde{\boldsymbol{x}} = \Omega'\hat{\boldsymbol{z}} \times (\tilde{\boldsymbol{x}} - \boldsymbol{C}), \tag{58}$$

[12] This can be seen also this way: the centre of mass of the rotor moves forward with velocity $\hat{\boldsymbol{y}}\Omega_{\text{rot}}R_{\text{rot}}$ and only this linear velocity has non-trivial component in the direction of the surface normal

where

$$\Omega' = \Omega + \Omega_{\text{rot}} = \Omega \frac{R_{\text{stat}}}{R_{\text{rot}}(0)}. \tag{59}$$

The joy of a fixed domain comes at a price of fictitious forces appearing in the dynamics (namely centrifugal and Coriolis [13]). Any particle of mass m is now subject to an extra force

$$\mathbf{F} = \mathbf{F}_{\text{cent}} + \mathbf{F}_{\text{Cor}}, \tag{60}$$

where [14]

$$\mathbf{F}_{\text{Cor}} = 2m\Omega\, \hat{\boldsymbol{z}} \times \tilde{\boldsymbol{u}} \tag{61}$$

and

$$\mathbf{F}_{\text{cent}} = -m\Omega^2 \hat{\boldsymbol{z}} \times (\hat{\boldsymbol{z}} \times \tilde{\boldsymbol{x}}) = m\nabla \left(\frac{1}{2} \Omega^2 r^2 \right) \tag{62}$$

(here $r = \sqrt{x^2 + y^2}$ is denoting the distance from the z-axis). This means that the Navier-Stokes equations (15) will have the following form:

$$\frac{\partial\, \tilde{\boldsymbol{u}}}{\partial\, t} + (\nabla \cdot \tilde{\boldsymbol{u}})\, \tilde{\boldsymbol{u}} = \boldsymbol{f} - \frac{1}{\rho} \nabla p + \nu \Delta \tilde{\boldsymbol{u}} + \nabla \left(\frac{1}{2} \Omega^2 r^2 \right) + 2\Omega \hat{\boldsymbol{z}} \times \tilde{\boldsymbol{u}}. \tag{63}$$

Let us assume that $\boldsymbol{f} = -\nabla\psi$, where ψ is the gravitational potential. It is now good time to introduce the *effective pressure* [15]:

$$P = \frac{p}{\rho} + \psi - \frac{1}{2} \Omega^2 r^2. \tag{64}$$

This allows us to simplify our equation considerably:

$$\frac{\partial\, \tilde{\boldsymbol{u}}}{\partial\, t} + (\nabla \cdot \tilde{\boldsymbol{u}})\, \tilde{\boldsymbol{u}} = -\nabla P + \nu \Delta \tilde{\boldsymbol{u}} + 2\Omega \hat{\boldsymbol{z}} \times \tilde{\boldsymbol{u}}. \tag{65}$$

Note that from a mathematician's point of view, P is just an unknown enforcing the incompressibility $\operatorname{div} \tilde{\boldsymbol{u}} = 0$. This eventually makes centrifugal and gravitational force somewhat irrelevant in the equations.

4.2 Dimensional analysis

In a theoretical analysis it can be sometimes convenient to neglect the viscous force density $\nu \Delta \boldsymbol{u}$. According to measurements, the kinematic viscosity of water at 20°C is [2]

$$\nu \approx 1.0035 \cdot 10^{-6} \mathrm{m}^2/\mathrm{s}. \tag{66}$$

[13] We do not consider the Euler force as we assume that the turbine operates steadily and thus Ω is constant.

[14] the sign is positive because the precession is clockwise

[15] Although it is not really pressure in the sense that the units are $\mathrm{m}^2/\mathrm{s}^2 = \mathrm{J/kg}$.

However, to say that 10^{-6} is a small number is not by itself a sufficient argument for neglecting the effects viscosity — it could happen, for example, that the expression (66) only appears small because meter is an impractically large dimension for the problem in question. To justify "smallness" properly, one has to compare the magnitude of viscous force against other terms which appear in the equation. To this end, we define the *characteristic length* L_{char} as square root of the cross sectional area at the point of contact between the rotor and the stator, i.e.

$$L_{\text{char}} = \sqrt{A} = \sqrt{\pi(R_{\text{stat}}(0)^2 - R_{\text{rot}}(0)^2)}. \tag{67}$$

Next, we define the *characteristic speed* U_{char} as the average inflow speed, i.e.

$$U_{char} = \frac{Q}{\rho A},$$

where Q is the total flux. It is then natural to fix the *characteristic time* as

$$T_{\text{char}} = \frac{L_{\text{char}}}{U_{\text{char}}} \tag{68}$$

and the *characteristic pressure* as

$$P_{\text{char}} = \rho U_{\text{char}}^2. \tag{69}$$

With these scales given, we can now introduce dimensionless equivalents of velocity, pressure and time

$$\hat{\boldsymbol{u}} = \frac{\tilde{\boldsymbol{u}}}{U_{\text{char}}}, \qquad \hat{t} = \frac{t}{T_{\text{char}}}, \qquad \hat{P} = \frac{P}{P_{\text{char}}} \tag{70}$$

as well as differential operators

$$\hat{\nabla} = L_{\text{char}}\,\nabla, \qquad \hat{\Delta} = L_{\text{char}}^2\,\Delta. \tag{71}$$

Now, we just multiply (65) by $L_{\text{char}}/U_{\text{char}}^2 = T_{\text{char}}/U_{\text{char}}$ to obtain:

$$\frac{\partial\,\hat{\boldsymbol{u}}}{\partial\,\hat{t}} + \left(\hat{\nabla}\cdot\hat{\boldsymbol{u}}\right)\hat{\boldsymbol{u}} = -\hat{\nabla}\hat{P} + \frac{\nu}{L_{\text{char}}U_{\text{char}}}\,\hat{\Delta}\hat{\boldsymbol{u}} + \frac{2\Omega L_{\text{char}}}{U_{\text{char}}}\,\hat{\boldsymbol{z}}\times\hat{\boldsymbol{u}}. \tag{72}$$

The fractions

$$\text{Re} = \frac{L_{\text{char}}U_{\text{char}}}{\nu}, \qquad \text{Ro} = \frac{U_{\text{char}}}{2\Omega L_{\text{char}}} \tag{73}$$

are the well known *Reynolds number* and the *Rossby number* respectively. Using these, we can rewrite the equation (72) as

$$\frac{\partial\,\hat{\boldsymbol{u}}}{\partial\,\hat{t}} + \left(\hat{\nabla}\cdot\hat{\boldsymbol{u}}\right)\hat{\boldsymbol{u}} = -\hat{\nabla}\hat{P} + \frac{1}{\text{Re}}\,\hat{\Delta}\hat{\boldsymbol{u}} + \frac{1}{\text{Ro}}\,\hat{\boldsymbol{z}}\times\hat{\boldsymbol{u}}. \tag{74}$$

High Reynolds number indicates flows, where viscous forces are weak. The lower the Rossby number, the stronger are the effects of Coriolis force. Note that negative values of Ro are permitted as switching the direction of precession also changes the sign of Coriolis force. On the other hand, the Reynolds number Re is always positive.

Based on dimensional analysis alone, it is possible to deduce that the formula for power on the turbine must be of the form

$$\dot{W} = \rho c L_{\text{char}}^4 \Omega^2 U_{\text{char}} = cAQ\Omega^2 \tag{75}$$

where the dimensionless "constant" c is actually an unknown function

$$c = c(\text{Re}, \text{Ro}).$$

The value c can be either negative (in this case, power has to be provided into the system and the fluid creates a stopping force) or positive (in which case, the fluid creates a positive feedback on the motion and power must be extracted from the system or else the rotor would begin to accelerate). Once the geometry and the boundary conditions are specified [16], this becomes a purely mathematical problem.

Problem. *Are there values of* $Re > 0$ *and* $Ro \in \mathbb{R}$ *such that the equation (74) permits a stationary solution with* $c > 0$*?*

The very fact the SETUR works indicates a positive answer, unless our mathematical description is incorrect. Constant c is to be calculated by comparing (75) with

$$\dot{W} = -\int_{\Gamma_{\text{rot}}} \mathbf{u} \cdot \mathbb{T}\mathbf{n} \, \mathrm{d}S, \tag{76}$$

where Γ_{rot} is the surface of rotor and $\mathbf{n}$ is the outward normal of the fluid domain Ω (i.e. inward with respect to the rotor). Note that this formula works only in the inertial frame of reference.

Another information that we can obtain is the so called *similarity of flows*: any two turbines with the same geometry but different sizes will exhibit the same behaviour as long as Re and Ro remain unchanged. For any $\lambda > 0$ the following transformation

$$L_{\text{char}} \mapsto \lambda L_{\text{char}}, \quad U_{\text{char}} \mapsto \lambda^{-1} U_{\text{char}}, \quad \Omega \mapsto \lambda^{-2}\Omega$$

does not[17] change Re or Ro. Therefore, it must be that the power generated by the fluid after the transformation must be

$$\rho c(\lambda L_{\text{char}})^4 (\lambda^{-2}\Omega)^2 (\lambda^{-1} U_{\text{char}}) = \lambda^{-1}\dot{W} \tag{77}$$

[16] This will be done in the section about numerical simulation.

[17] with the kinematic viscosity and density being the same

On first glance, this appears to be nonsensical, as we would get that a ten times smaller turbine could generate ten times greater power. Since the flux Q is U_{char} divided by inflow area, it would also be ten times smaller. Does it mean that we should build our rolling turbines as small as possible? The mistake in this type of reasoning is that one must also take into account the amount of pressure needed to transport the fluid through the turbine. By definition, the efficiency of the turbine is

$$\eta = \frac{\dot{W}}{gQH}, \tag{78}$$

where H is the hydraulic head. Since η is a dimensionless parameter, there also must be a dependence

$$\eta = \eta(\mathrm{Re}, \mathrm{Ro}).$$

Naturally, geometrically similar turbines will operate at the same efficiency. Thus, the ten times smaller turbine would require hundred times greater hydraulic head to operate with the given flux and precession angular velocity.

In article [1], experimental data for two different SETURs are provided: in one case, the rotor is a truncated cone and in the other case, it is a sphere. For each of those, the table below lists the relevant data as well as the calculated Reynolds and Rossby numbers. (The angular velocity is related to the rolling frequency by $\Omega = 2\pi f$. In both cases, the values $\rho = 1000\,\mathrm{kg/m^3}$ and $\nu = 1.0035 \cdot 10^{-6}\mathrm{m^2/s}$ were used.)

	R_{stat}	R_{rot}	f	Q	Re	Ro	c
truncated cone	0.135 m	0.125 m	3.7 Hz	3.2 kg/s	35283	0.093	0.446
sphere	0.071 m	0.061 m	6.3 Hz	4.2 kg/s	64994	0.151	0.326

What we see is that the Reynolds number for this problem is quite large (in the order of tens of thousand) and so the flow will be dominated by convection rather than by viscosity. On the other hand, the Coriolis force is comparable to convection and thus, based on this analysis alone, it cannot be neglected.

4.3 Flow in a thin annular channel

We will now attempt to explain analytically the principle behind functionality of the rolling turbine. Unfortunately, the full scale three dimensional problem is extremely complicated — it must either include Coriolis force, when treated in a co-precessing frame, or be a non-steady problem with variable geometry, when

treated in an inertial frame. Trying to solve such a problem analytically would be merely a waste of time. Thus, without resorting to heavy numerical methods, we can provide an analysis only under several layers of approximation. We believe that a simplified analytical explanation might shed more light on the principles behind the turbine than results of a complex numerical simulation.

As demonstrated in (4), the force which acts on the rotor can be decomposed into it's normal pressure component $\boldsymbol{G}_p = p\boldsymbol{n}$ and the tangential component $\boldsymbol{G}_\nu = -2\rho\nu\mathbb{D}\boldsymbol{n}$ associated with the viscosity. Since the rotor performs both rotary as well as linear motion, both of these forces may potentially generate power. We propose that the main driving force is the pressure field. This is for two reasons: Firstly the rotor can operate in the presence of vortex going against the direction of the rolling motion, where the power due to viscous force must be negative and secondly, in all performed numerical simulations (which will be described later), direct viscous effects were very small. The total power of pressure field on the conical rotor B at $t = 0$ can be evaluated from the inertial frame as

$$\dot{W} = \int_{\partial B} -p\boldsymbol{n}\cdot\boldsymbol{u} = \int_{\partial B} -pu_{\boldsymbol{n}} = -\sqrt{1+\gamma^2}\int_{-h}^{0}\int_{-\pi}^{\pi} pu_{\boldsymbol{n}}R_{\mathrm{rot}}(z)\,\mathrm{d}\theta'\,\mathrm{d}z, \tag{79}$$

where h is the height of the rotor. Using (55), this yields:

$$\begin{aligned}\dot{W} &= -R_{\mathrm{rot}}(0)\Omega_{\mathrm{rot}}\int_{-h}^{0} R_{\mathrm{rot}}(z)\left(\int_{-\pi}^{\pi} p\sin\theta'\,\mathrm{d}\theta'\right)\,\mathrm{d}z.\\ &= -\Omega^2 d\int_{-h}^{0} R_{\mathrm{rot}}(z)\left(\frac{1}{\Omega}\int_{-\pi}^{\pi} p\sin\theta'\,\mathrm{d}\theta'\right)\,\mathrm{d}z.\end{aligned} \tag{80}$$

In order to get a positive feedback of the flow on precession (regardless of the sign of Ω), we would need to have

$$\frac{1}{\Omega}\int_{-\pi}^{\pi} p\sin\theta'\,\mathrm{d}\theta' < 0 \tag{81}$$

that is, the power is associated with the negative sine moment of pressure near $z = 0$. We derive this inequality for a brutally simplified problem in the geometry between two coaxial cylinders

$$U = \{(r,\theta,z), R_{\mathrm{stat}} < r < R_{\mathrm{rot}}\} \tag{82}$$

but with θ-dependant inlet velocity such as to match the θ-distribution of flux of the original moon-shaped cross-section (see figure (3)). The idea is that the variation in the inflow velocity will interact with a fictitious solid body vortex, that exists due to the frame being non-inertial. This interaction leads to the formation of a pressure field such that the inequality (81) holds (where, in our

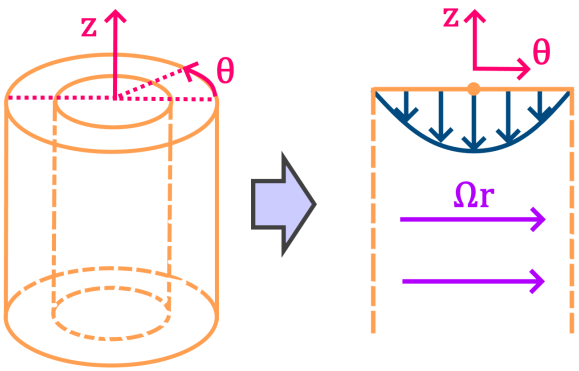

Figure 4: Reduction into a two-dimensional problem

simplified concentric problem $\theta = \theta'$). The Navier-Stokes equations in the co-precessing frame with respect to cylindrical coordinates[18] are (see (65) and the appendix):

$$\begin{aligned} \dot{u}_r - \frac{u_\theta^2}{r} &= -\frac{\partial P}{\partial r} + \nu \left\{ \Delta u_r - \frac{2}{r^2}\frac{\partial u_\theta}{\partial \theta} - \frac{u_r}{r^2} \right\} - 2\Omega u_\theta, \\ \dot{u}_\theta + \frac{u_r u_\theta}{r} &= -\frac{1}{r}\frac{\partial P}{\partial \theta} + \nu \left\{ \Delta u_\theta + \frac{2}{r^2}\frac{\partial u_r}{\partial \theta} - \frac{u_\theta}{r^2} \right\} + 2\Omega u_r, \\ \dot{u}_z &= -\frac{\partial P}{\partial z} + \nu \Delta u_z \end{aligned} \tag{83}$$

and

$$\frac{\partial u_r}{\partial r} + \frac{1}{r}\frac{\partial u_\theta}{\partial \theta} + \frac{\partial u_z}{\partial z} + \frac{u_r}{r} = 0. \tag{84}$$

where (assuming that the flow is steady):

$$\dot{\varphi} = \frac{\partial \varphi}{\partial r} u_r + \frac{1}{r}\frac{\partial \varphi}{\partial \theta} u_\theta + \frac{\partial \varphi}{\partial z} u_z, \tag{85}$$

for any continuously differentiable function φ. Now we further simplify the equations by neglecting the viscosity, assuming $u_r \approx 0$, and investigate the equations for θ and z in the proximity of the rotor at $r = R_{\text{rot}}$. This leads to a set of two

[18] we decided to no longer denote velocity in the co-precessing frame with tilde because it would be highly annoying to type and read. In this subsection, all computations are made in this frame.

equations[19]:

$$\begin{aligned} \frac{1}{R_{\text{rot}}}\frac{\partial u_\theta}{\partial \theta}u_\theta + \frac{\partial u_\theta}{\partial z}u_z &= -\frac{1}{R_{\text{rot}}}\frac{\partial P}{\partial \theta}, \\ \frac{1}{R_{\text{rot}}}\frac{\partial u_z}{\partial \theta}u_\theta + \frac{\partial u_z}{\partial z}u_z &= -\frac{\partial P}{\partial z} \end{aligned} \tag{86}$$

in the two-dimensional domain $[\theta, z] \in (-\pi, \pi) \times (-\infty, 0)$. We complement this by the following boundary conditions:

$$u_z|_{z=0} = u_{\text{in}} = -u_0 - u', \qquad \text{(inflow)}$$

$$\left.\begin{pmatrix} u_\theta \\ u_z \end{pmatrix}\right|_{\theta=\pi} = \left.\begin{pmatrix} u_\theta \\ u_z \end{pmatrix}\right|_{\theta=-\pi}, \qquad \text{(periodicity)}$$

$$\lim_{z\to-\infty}\begin{pmatrix} u_\theta \\ u_z \end{pmatrix} = \begin{pmatrix} \Omega R_{\text{rot}} \\ -u_0 \end{pmatrix}. \qquad \text{(flow at infinity)}$$

Here,

$$u_0 = \frac{Q}{\rho A} \tag{87}$$

denotes the average inflow in z direction and $u'(\theta)$ is the deviation from this average, which we will assume to be an even function of θ. The condition at infinity is to exclude non-physical solutions that diverge as $z \to -\infty$. Now, we search for a solution in the form of a potential flow

$$\begin{pmatrix} u_\theta \\ u_z \end{pmatrix} = \begin{pmatrix} \Omega R_{\text{rot}} \\ -u_0 \end{pmatrix} + \nabla\varphi = \nabla\left(\Omega R_{\text{rot}}^2\theta - u_0 z + \varphi\right) \tag{88}$$

where $\varphi(\theta, z)$ is an unknown velocity potential and we denote

$$\nabla\varphi = \begin{pmatrix} \frac{1}{R_{\text{rot}}}\frac{\partial\varphi}{\partial\theta} \\ \frac{\partial\varphi}{\partial z} \end{pmatrix}. \tag{89}$$

Just like in the case of classical Bernoulli equation (29), the irrotationality [20] allows us to rewrite (86) as

$$\nabla\left(\frac{u^2}{2} + P\right) = 0 \tag{90}$$

[19]Note that the Coriolis force vanishes from the system, since it's only component affecting $\mathbf{u}_z$ or $\mathbf{u}_\theta$ is the one which is proportional to u_r

[20]with respect to θ, z

or

$$\frac{u^2}{2} + P = \text{const.} \tag{91}$$

Now, the condition of incompressibility (84) leads to a Laplace equation

$$\frac{1}{R_{\text{rot}}^2}\frac{\partial^2 \varphi}{\partial \theta^2} + \frac{\partial^2 \varphi}{\partial z^2} = 0. \tag{92}$$

This can be solved easily using the Fourier's method. Firstly, let us decompose u' into a cosine series [21]:

$$u'(\theta) = u_0 \sum_{k=1}^{\infty} a_k \cos k\theta. \tag{93}$$

The crucial idea is that we expect the inflow to be largest in magnitude at $\theta = 0$ and monotonically diminish at the edges $\theta = \pm\pi$ (As corresponding to the original geometry. This is actually the only place where viscosity is indirectly taken into account — at $z = 0$ where the gap between stator and rotor is smallest.) Mathematically, this means that it is reasonable to expect

$$a_1 = \frac{1}{\pi u_0}\int_{-\pi}^{\pi} u'(\theta)\cos\theta \,\mathrm{d}\theta > 0.$$

Next, we search for φ in the form

$$\varphi(\theta, z) = \sum_{k=1}^{\infty} b_k(z)\cos k\theta. \tag{94}$$

Substituting this into (92) and comparing individual nodes gives as an ordinary differential equation for coefficients b_k:

$$-\frac{k^2}{R_{\text{rot}}^2}b_k + \frac{\mathrm{d}^2 b_k}{\mathrm{d}\, z^2} = 0, \qquad \frac{\mathrm{d}\, b_k}{\mathrm{d}\, z}(0) = -u_0 a_k, \qquad \lim_{z\to-\infty}\frac{\mathrm{d}\, b_k}{\mathrm{d}\, z} = 0. \tag{95}$$

This leads to a solution

$$b_k(z) = -\frac{u_0 R_{\text{rot}} a_k}{k}\,\exp\left(\frac{kz}{R_{\text{rot}}}\right). \tag{96}$$

Putting this into (94), we obtain

$$\varphi = -u_0 R_{\text{rot}} \sum_{k=1}^{\infty}\frac{a_k}{k}\exp\left(\frac{kz}{R_{\text{rot}}}\right)\cos k\theta \tag{97}$$

[21] Sine nodes do not appear here, because on the basis of the symmetry of the inflow, we assume that u' is even in θ.

and

$$\begin{pmatrix} u_\theta \\ u_z \end{pmatrix} = \begin{pmatrix} \Omega R_{\text{rot}} \\ -u_0 \end{pmatrix} + u_0 \sum_{k=1}^{\infty} a_k \begin{pmatrix} \sin k\theta \\ -\cos k\theta \end{pmatrix} \exp\left(\frac{kz}{R_{\text{rot}}}\right). \tag{98}$$

Hence, we calculate:

$$\begin{aligned} \frac{u^2}{2} &= \frac{1}{2}\left[\Omega R_{\text{rot}} + u_0 \sum_{k=1}^{\infty} a_k \sin k\theta \, \exp\left(\frac{kz}{R_{\text{rot}}}\right)\right]^2 \\ &\quad + \frac{1}{2}\left[u_0 + u_0 \sum_{k=1}^{\infty} a_k \cos k\theta \, \exp\left(\frac{kz}{R_{\text{rot}}}\right)\right]^2 \end{aligned} \tag{99}$$

and

$$\begin{aligned} \int_{-\pi}^{\pi} \frac{u^2}{2} \sin\theta \, \mathrm{d}\theta &= \int_{-\pi}^{\pi} \Omega R_{\text{rot}} u_0 a_1 \sin^2\theta \, \exp\left(\frac{z}{R_{\text{rot}}}\right) \, \mathrm{d}\theta \\ &= \pi \Omega R_{\text{rot}} u_0 a_1 \exp\left(\frac{z}{R_{\text{rot}}}\right). \end{aligned} \tag{100}$$

Let us assume that the gravitational potential ψ does not depend on θ (such as when the gravitational force points in the $-\hat{\boldsymbol{z}}$ direction). Then finally, we obtain

$$\begin{aligned} -\frac{1}{\Omega}\int_{-\pi}^{\pi} p \sin\theta \, \mathrm{d}\theta &= -\frac{\rho}{\Omega}\int_{-\pi}^{\pi} \left(P - \psi + \frac{1}{2}\Omega^2 R_{\text{rot}}^2\right) \sin\theta \, \mathrm{d}\theta \\ &= \frac{\rho}{\Omega}\int_{-\pi}^{\pi} \frac{u^2}{2} \sin\theta \, \mathrm{d}\theta \\ &= \pi \rho R_{\text{rot}} a_1 u_0 \exp\left(\frac{z}{R_{\text{rot}}}\right) > 0 \end{aligned} \quad . \tag{101}$$

One natural choice is to set

$$u_{\text{in}} = -\frac{Q}{\rho A}\left(1 + \cos\theta\right). \tag{102}$$

Then $a_1 = 1$ and the solution becomes (see figure (5))

$$\begin{pmatrix} u_\theta \\ u_z \end{pmatrix} = \begin{pmatrix} \Omega R_{\text{rot}} + u_0 \, e^{z/R_{\text{rot}}} \sin\theta \\ -u_0 - u_0 \, e^{z/R_{\text{rot}}} \, \cos\theta \end{pmatrix}. \tag{103}$$

The presented analysis has, of course, many limitations. To begin with, omitting the viscosity is extremely problematic near the surface of the rotor, even with $\mathrm{Re} \gg 1$ — this is because in the boundary layer, the second derivatives in $\Delta \boldsymbol{u}$ may become very large. (Although, as will be shown later, our numerical computations

suggest that viscous power is still smaller by several orders of magnitude since the differences in tangential velocities are not so large.) Secondly, the assumption of the irrotationality of flow in (86), under which Bernoulli's equation is applied, is rather ill-supported. (We will show later that the assumption of irrotationality is not essential.)

Nonetheless, using the assumption above, our analysis indicates how SETUR might work:

1. Since the rotor's position deviates from the central symmetry axis, the flux goes primarily where the cross section is greatest (this is, where viscosity must be taken into account).

2. Shape of the rotor is such that the cross section in the wider and the thinner part tend to equalize. By incompressibility, this would make the flow slower in the initially thinner region.

3. However, water tends to equalize this difference. From the co-precessing frame, this generates a secondary flow, which then interacts with the fictitious vortex, generating a pressure field. (From the inertial frame, periodic temporal changes in flux would cause non-zero divergence. Since the water is practically incompressible, a secondary flow must appear and this is accompanied with generation of a pressure field.)

4. This pressure field acts as a positive feedback on the rotor and can be used to generate power.

Naive substitution of this solution into 80 would yield a power formula

$$\dot{W} = cAQ\Omega^2, \tag{104}$$

where

$$c = \frac{\pi d}{A^2} \int_{-h}^{0} R_{\mathrm{rot}}^2(z) \exp\left(\frac{z}{R_{\mathrm{rot}}(z)}\right) \tag{105}$$

is an actual constant. Such equation would not, however, take into account friction. Therefore, we suggest a corrected formula in the form

$$c = a - \frac{b}{|\mathrm{Ro}|}, \tag{106}$$

where a, b are constant dimensionless parameters. This is motivated by the fact

that letting $Q \to 0$ reduces the equation

$$\begin{aligned} \dot{W} &= \left(a - \frac{b}{|\mathrm{Ro}|}\right) AQ\Omega^2 \\ &= \left(a - \frac{2b\rho A^{3/2}|\Omega|}{Q}\right) AQ\Omega^2 \end{aligned} \tag{107}$$

into

$$\dot{W} = -2b\rho A^{5/2}|\Omega|^3 \tag{108}$$

which corresponds to the Newton's drag formula [22] [23]. This is also in a reasonable agreement with the experiments, see figure (6).
As a remark, the hydraulic principle described above can be also easily understood without resorting to Bernoulli's equation and to the assumption of irrotationality. An alternative approach is to prescribe both: θ-dependant velocity u_z and a constant axial velocity u_θ at the inflow. If there was no pressure affecting the fluid particles, these particles would simply follow their *convection lines* - i.e. lines of constant velocity extended from $z = 0$ (This corresponds to a solution of the inviscid Burgers' equation). One would then obtain lines that converge on one side and diverge on the other. If we now imagine that water is slightly compressible (which it actually is), we see that this should cause variations in density and consequently also in the pressure.

As another remark, the described principle was derived assuming off-centred position of the rotor, being a reaction to the orbital movement. We suggest, however, that this mechanism is somewhat more general and is applicable to many different types of motion of the rotor within the fluid. Whenever the rotor moves, it creates variations in the flow field (which is due to viscosity and due to the converging geometry of the rotor — hemisphere or cone) and leads to the drag inversion. This is in analogy with our analysis, when it is understood from the inertial frame of reference (then, there is no "fictitious" vortex but periodically time-dependant inflow instead). However, these effects seem to be significant only when the gap d is very small. (As observed by ing. Sedláček, the rolling turbine simply does not work when the gap is too large.) In frame of our analysis, this can be explained as a necessity of having a cross-section where viscous forces are the dominating force in the equations.

[22] By Newton's formula, drag force should be proportional to Ω^2. The power of friction is then proportional to Ω^3.

[23] It should be noted that even without the addition of drag, the runaway positive feedback ($|\Omega| \to \infty$) does not violate the conservation of mechanical energy. This is because in the analysis, we assume sufficiently large hydraulic head H, which is increased together with Ω. This effect seems to be related to the application of rolling turbine as a hydraulic pump. The dependence of H on Ω is still not completely understood by the author

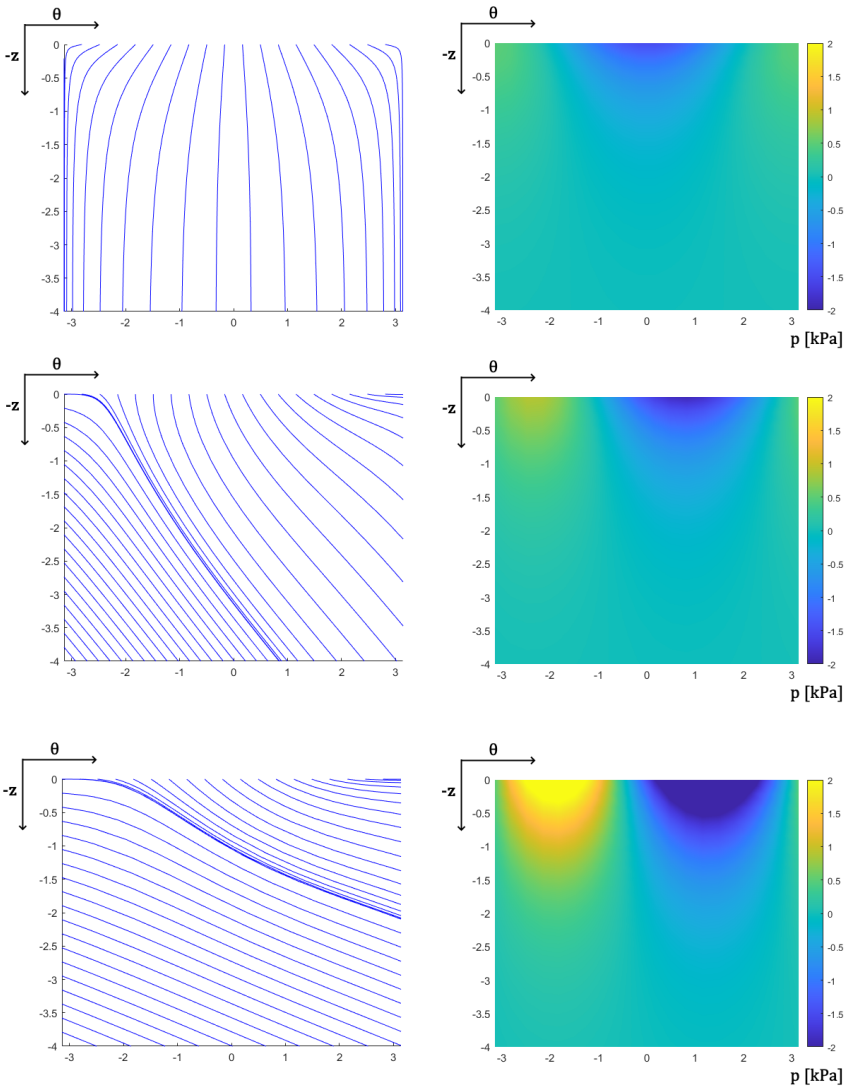

Figure 5: In these Matlab figures are plotted the streamlines and the pressure distribution for $u_0 = 1$ m/s and for $\Omega R_{\text{rot}} = 0, 1, 3$ m/s (from top to down). The pressure is measured in kPa. It can be seen that as Ω increases, the pressure becomes notably asymmetric with respect to θ. The pressure is greater at $\theta < 0$, which corresponds to the rear side of the rotor.

4.4 Vortex interaction

The formula (107) was derived under the assumption that the angular momentum at the inflow was zero — there was only a fictitious vortex of angular speed Ω due to analysis being done in a co-precessing frame (in the inertial frame there would

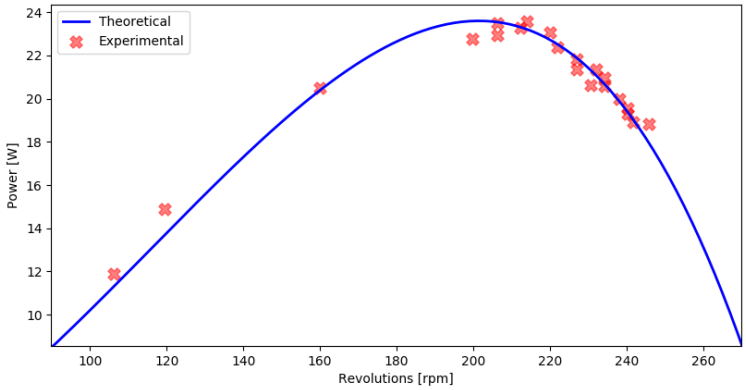

Figure 6: Comparison of the formula 107 with experimental data. Only the dependence on Ω for fixed Q was tested. Free parameters a, b were fitted using the method of least squares. The data were obtained from [4]

be no vortex, but the inflow condition would be periodically time-dependant). In practise, however, the stream can be ducted tangentially (from a side) such that water begins to whirl before entering the turbine. Arguably the most intriguing property of SETUR is that the rotor can roll both in or against the direction of this vortex. As mentioned earlier, the obtainable power is greater when the precession goes in the *same* direction as the vortex (i.e. for real vortex being opposite to the fictitious vortex). Let us show that this is in accordance with our analysis. Suppose that in 86 we instead prescribed

$$u_\theta = R_{\text{rot}}(\Omega - \vartheta)$$

as a condition at $-\infty$, where ϑ is the magnitude of the (real) vortex and which is assumed to be constant. Then, by following the same arguments, the obtained power would be of the form

$$\dot{W} = \left(a - \frac{2b\rho A^{3/2}}{Q}|\Omega - \vartheta|\right) AQ(\Omega - \vartheta)\Omega. \tag{109}$$

This can alternatively written as

$$\dot{W} = B\,\hat{\Omega}(\hat{\Omega} - \hat{\vartheta})\left(1 - |\hat{\Omega} - \hat{\vartheta}|\right), \tag{110}$$

where

$$\hat{\Omega} = \frac{2b\rho\sqrt{A}}{aQ}\,\Omega\,, \qquad \hat{\vartheta} = \frac{2b\rho\sqrt{A}}{aQ}\,\vartheta\,, \qquad B = \frac{a^3Q^3}{4b^2\rho^2A^2}\,.$$

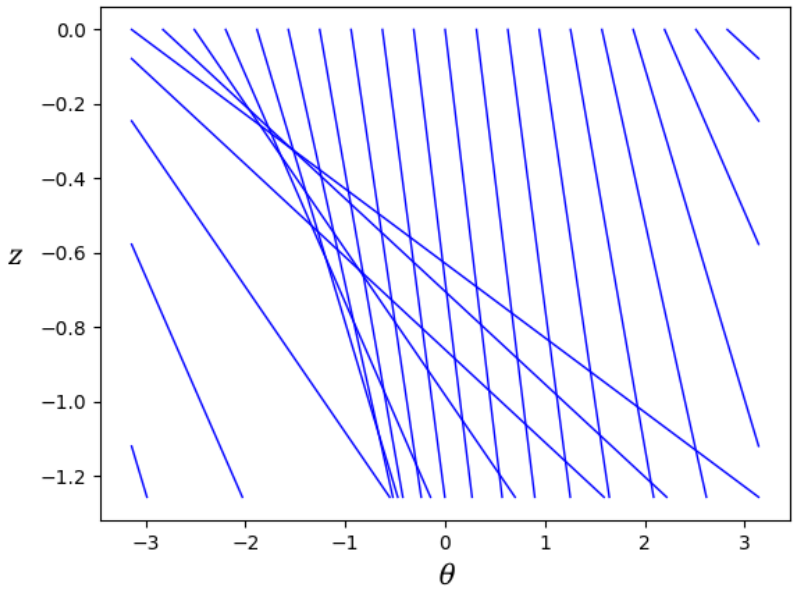

Figure 7: Convection lines that would converge in the rear region $\theta < 0$ and diverge in the front region $\theta > 0$. Strong pressure forces in the fluid prevent this compression, which results in a θ-dependant pressure field.

Then, it is an easy exercise to calculate that for every fixed $\hat{\vartheta} \in (0, 1)$, the maximum power is attained for $\hat{\Omega} \in (\hat{\vartheta}, 1 + \hat{\vartheta})$ and satisfies (for $\hat{\vartheta}$ close to 0)

$$\dot{W}_{\max}(\hat{\vartheta}) = \frac{B}{27}\big(4 + 6\hat{\vartheta}\big) + O\big(\hat{\vartheta}^2\big).$$

Hence, adding a vortex that goes in the direction of Ω increases the maximum attainable power.

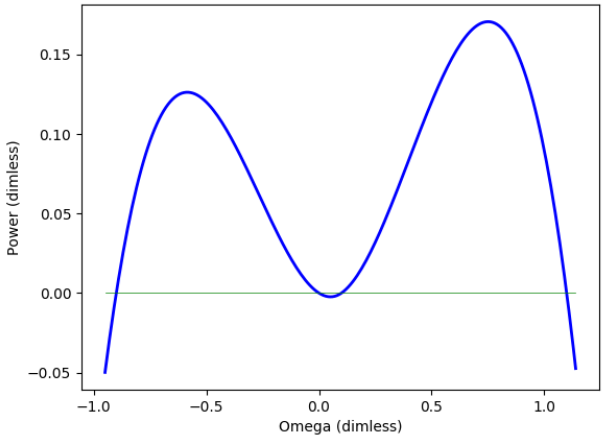

Figure 8: The graph of the function $\dot{W}/B$ with respect to $\hat{\Omega}$ for fixed $\hat{\theta} = 0.1$. Note that the right bulge is higher. Thus the maximum attainable power is higher when the rolling goes in the direction of the vortex.

4.5 The emergence of rolling motion

As discussed in (4.3), operation of the rolling turbine can be explained via non-linear interaction between the transversal flux and the flow induced due the movement of the rotor itself. As a consequence of Bernoulli's principle, this produces a forward pulling force, resulting in a drag inversion and hence instability. For high orbital velocities, this force is eventually counter-acted by friction, which has higher asymptotic rate in rotor's velocity (quadratic or greater). So far, we have only analysed this as a stationary effect: the rotor was *prescribed* to precede with the given angular velocity Ω and the power output from the rotor was measured. We deem this approach not completely satisfactory as it does not answer this important question:

Problem. *Is the steady configuration stable? How does it emerge from the initial concentric configuration?*

It would be very ambitious to analyse this problem in it's fullest scale, i.e. using non-stationary Navier-Stokes equations coupled with the rotor's solid body motion in a moving geometry[24]. We will not undertake this direction here. Instead, we shall try to approximate dynamical behaviour using a set of ordinary differential

[24]Although, we think it should be possible to do numerically, using a combination of the co-precessing frame and an ALE method to account for the radial motion of the rotor.

equations with collision discontinuities.[25] The aim of this effort is to show that inverted drag, when generalized to non-orbital motions, serves not only as an explanation of initial instability, but also explains the transition from the initial to the rolling configuration. To this end, let

$$\boldsymbol{x} = \begin{pmatrix} x \\ y \end{pmatrix}, \qquad \boldsymbol{v} = \begin{pmatrix} v_x \\ v_y \end{pmatrix}$$

be the coordinates of the rotor's axis in the $z = 0$ plane and its velocity respectively. Let us assume that when the rotor is not touching stator, the velocity is subject to a differential equation:

$$\frac{\mathrm{d}\boldsymbol{v}}{\mathrm{d}t} = F(v)\boldsymbol{v}, \tag{111}$$

where $F : [0, +\infty) \to \mathbb{R}$ is a locally Lipschitz continuous function satisfying $F(0) = 0$. Further suppose that there exists some limit velocity $V > 0$ such that

$$\begin{aligned} &F(v) > 0, \quad v \in (0, V), && \text{(drag is invertion)} \\ &F(v) < 0, \quad v \in (V, +\infty). && \text{friction dominates} \end{aligned}$$

This means that any static configuration is unstable. An arbitrarily small perturbation of $\boldsymbol{v}$ will cause the rotor to accelerate along a straight line with v approaching V asymptotically.[26] Transforming (111) into polar coordinates $r\theta$, we obtain:

$$\begin{aligned} \frac{\mathrm{d}v_r}{\mathrm{d}t} &= F(v)v_r + \frac{v_\theta^2}{r}, \\ \frac{\mathrm{d}v_\theta}{\mathrm{d}t} &= F(v)v_\theta - \frac{v_r v_\theta}{r}. \end{aligned} \tag{112}$$

At $r = d := R_{\mathrm{stat}} - R_{\mathrm{rot}}$ is when the rotor collides with the stator. We will assume an inelastic collision, such that

$$v_r \mapsto -\alpha v_r, \tag{113}$$

where $\alpha \in (0, 1)$ is the *coefficient of restitution*. It remains to determine what happens with v_θ during a collision. Let G be the tangential component of the impulse of force by which the stator acts on the rotor at the point of contact. This impulse will cause a discontinuous change in v_θ:

[25] This will be somewhat similar to the well known problem of *billiards*, see [14]. The major difference will be that in our case non-elastic collisions will be considered,

[26] Both F and V have additional dependence on the transversal flux Q which is assumed to be constant. Still, this is only a crude approximation and plethora of additional dependencies might be considered. Namely those on: the actual position $\boldsymbol{x}$, the acceleration $\boldsymbol{a}$ or even the full history of motion.

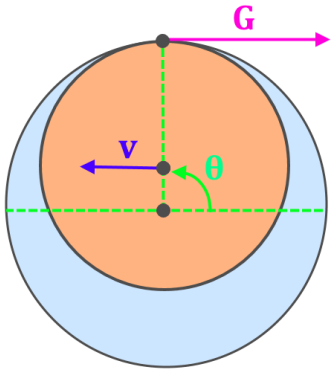

Figure 9: The contact force G enforces no-slip when $r = d$.

$$v_\theta \mapsto v_\theta + \frac{G}{m_{\text{rot}}} \tag{114}$$

where m_{rot} is the mass of the rotor. At the same time, the impulse has a non-trivial moment, which results in a change of angular speed Ω_{rot}:

$$\Omega_{\text{rot}} \mapsto \Omega_{\text{rot}} + \frac{R_{\text{rot}} G}{I_{\text{rot}}} \tag{115}$$

where I_{rot} is the rotor's moment of inertia around its symmetry axis. The value of G can be determined by assuming no-slip contact after the collision. That gives

$$v_\theta + \frac{f}{m_{\text{rot}}} + R_{\text{rot}} \left(\Omega_{\text{rot}} + \frac{R_{\text{rot}} G}{I_{\text{rot}}} \right) = 0$$

$$G = -\frac{v_\theta + \Omega_{\text{rot}} R_{\text{rot}}}{\frac{1}{m_{\text{rot}}} + \frac{R_{\text{rot}}^2}{I}}$$

Let us introduce a dimensionless parameter $\beta = m_{\text{rot}} R_{\text{rot}}^2 / I_{\text{rot}}$. Plugging this into (114), (115), we obtain:

$$\begin{aligned} v_\theta &\mapsto v_\theta - \frac{v_\theta + \Omega_{\text{rot}} R_{\text{rot}}}{1+\beta}, \\ \Omega_{\text{rot}} &\mapsto \Omega_{\text{rot}} - \frac{\beta}{R_{\text{rot}}} \frac{v_\theta + \Omega_{\text{rot}} R_{\text{rot}}}{1+\beta}. \end{aligned} \tag{116}$$

To close this system, we must add a differential equation for Ω_{rot}. For that, we shall assume

$$\frac{\mathrm{d}\Omega_{\text{rot}}}{\mathrm{d}t} = -\kappa \Omega_{\text{rot}} \tag{117}$$

where $\kappa > 0$ is a coefficient which accounts for the skin friction on the rotor. Wrapping this up, we have a first-order system of five unknowns: r, θ, v_r, v_θ, Ω and five differential equations: (112), (117) and $\dot{r} = v_r$, $\dot{\theta} = v_\theta / r$ with jumps at $r = d$ described by (113), (116). Standard theory of ordinary differential systems

can be used to prove the existence and uniqueness of globally defined solutions for any initial data satisfying $r < d$.[27] Our wish is to show that for almost every initial configuration the solution will be attracted towards orbital motion, that is

$$r \to d \quad \text{and} \quad v_r \to 0 \quad \text{for} \quad t \to +\infty.$$

From equation (112), we easily get that

$$\begin{aligned} \frac{\mathrm{d}v^2}{\mathrm{d}t} &= 2F(v)v^2, \\ \frac{\mathrm{d}(rv_\theta)}{\mathrm{d}t} &= F(v)(rv_\theta) \end{aligned} \tag{118}$$

It is then a matter of a (rather long) discussion to show that the sets:

$$\begin{aligned} U^+ &= \{0 < +\Omega_{\mathrm{rot}} R_{\mathrm{rot}} \leq -v_\theta \leq v \leq V\} \\ U^- &= \{0 < -\Omega_{\mathrm{rot}} R_{\mathrm{rot}} \leq +v_\theta \leq v \leq V\} \end{aligned}$$

are positively invariant and that for almost every initial configuration, the solution enters one of those sets in finite amount of time. (One has to first show that $v > V$ causes an exponential decay of energy through collisions. Once $v < V$, after one subsequent collision, the solution enters one of the sets U^+ or U^- which it may never leave.) We can, therefore, with no loss of generality, assume only initial configurations in the set U^+. Next, we define dimensionless variables:

$$\xi = -\frac{\Omega_{\mathrm{rot}} R_{\mathrm{rot}} d}{r v_\theta}, \qquad \zeta = \frac{v^2 d^2}{r^2 v_\theta^2} - 1.$$

We see that $\xi \in (0, 1]$ and $\zeta \in (0, \infty)$. Using (118), we compute

$$\frac{\mathrm{d}\zeta}{\mathrm{d}t} = \frac{d^2}{r^2 v_\theta^2} \frac{\mathrm{d}v^2}{\mathrm{d}t} - \frac{2v^2 d^2}{r^3 v_\theta^3} \frac{\mathrm{d}(rv_\theta)}{\mathrm{d}t} = 0,$$

hence ζ is an integral of motion. The discontinuous jump in ζ during a collision is

[27] This analysis is better done using Cartesian coordinates. A slight problem might occur with solutions crossing the origin where polar coordinates are undefined. We may without loss of generality exclude these solutions from our discussion.

$$\begin{aligned}\Delta\zeta &= \Delta\left(\frac{v_r^2}{v_\theta^2}\right)\\ &= \left(\frac{(v_r+\Delta v_r)^2}{(v_\theta+\Delta v_\theta)^2}-\frac{v_r^2}{v_\theta^2}\right)\\ &= \frac{v_r^2}{v_\theta^2}\left[\left(\frac{1+\frac{\Delta v_r}{v_r}}{1+\frac{\Delta v_\theta}{v_\theta}}\right)^2-1\right]\\ &= -\zeta\left[1-\left(\frac{\alpha}{1-\frac{1-\xi}{1+\beta}}\right)^2\right].\end{aligned} \tag{119}$$

Now, let us denote t_k the times of individual collisions[28] and define:

$$\xi_k = \xi(t_{k+1}^-), \qquad \zeta_k = \zeta(t_k^+).$$

Then, using (119), we obtain the following difference relation:

$$\zeta_{k+1} = \alpha^2\left(\frac{1+\beta}{\xi_k+\beta}\right)^2\zeta_k \tag{120}$$

We can deduce that for

$$\alpha < \frac{\beta}{1+\beta}, \tag{121}$$

the sequence ζ_k will converge to zero as fast as a geometric sequence. Looking at the definition of ζ, this is only possible when $r \to d$ and $v_r \to 0$. In case of a solid hemispherical rotor, we have $\beta = 5/2$ and (121) leads to

$$\alpha < \frac{5}{7}.$$

In case of a thin hemispherical shell ($\beta = 3/2$), this would yield a slightly worse condition

$$\alpha < \frac{3}{5}.$$

We also see that if ξ_k are close to one, the converge may occur even when (121) is not satisfied. Note that $\xi = 1$ after each collision and ξ has a decay described by the equation

$$\frac{\mathrm{d}\xi}{\mathrm{d}t} = -\left[\kappa + F(v)\right]\xi. \tag{122}$$

[28] Since v may never completely vanish, there will be infinitely many such collisions.

The converge will then occur (regardless of "bad" β) provided that the rotor will move with sufficient rapidity. For suppose that we had some estimate of the type

$$\liminf_{t\to+\infty} v \geq \overline{v} > 0$$

valid for large t. Then (122) provides an estimate

$$\liminf \xi_k \geq \exp\left(-\frac{2d}{\overline{v}}\left[\kappa + \max_{v\geq\overline{v}} F(v)\right]\right) =: \overline{\xi}$$

and we get the following improvement of (121):

$$\alpha < \frac{\overline{\xi}+\beta}{1+\beta}. \tag{123}$$

This can be also observed in numerical experiments. There, we prescribed

$$F(v) = \gamma(V - v) \tag{124}$$

where $\gamma > 0$ was fixed. It was observed that starting from the concentric configuration (under some small perturbation), the rotor will first begin to bounce off the stator (moving mostly in radial direction) and then transition into an orbital rolling motion. Setting very high κ and α close to one prevented this transition. It is also possible to add a spring-like centripetal force, more precisely, to replace the r-equation in 112 by

$$\frac{\mathrm{d}v_r}{\mathrm{d}t} = F(v)v_r + \frac{v_\theta^2}{r} - kr, \tag{125}$$

where $k > 0$ is constant. Even with this centripetal force, the system would still converge to orbital motion. This transition is also associated with the decrease of energy loss per collision, which is in accordance with the principle of minimization of entropy production [9], see figure bellow. To conclude, centrifugal fluid force is not necessary to explain the transition from initial configuration — an inverted drag force is sufficient. The orbital motion is then (for wide range of parameters) the only stable solution and is self-emergent.

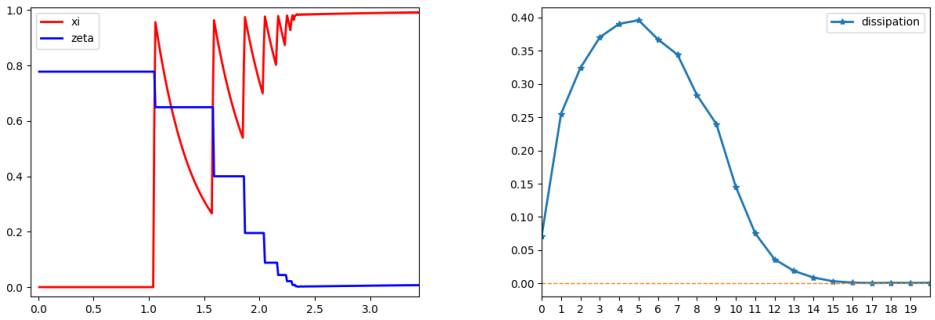

Figure 10: Values computed numerically. On the left, we see the evolution of ζ and ξ. On the right, we see the graph of dissipated energy at n-th collision. This analysis was only qualitative and dimensionless.

5 Simulation

5.1 Weak formulation

To use the method of finite elements, we must work with the *weak* formulation of incompressible Navier-Stokes equations. We remind that the classical formulation reads

$$\frac{\partial \boldsymbol{u}}{\partial t} + (\nabla \cdot \boldsymbol{u})\,\boldsymbol{u} = \boldsymbol{f} + \frac{1}{\rho}\operatorname{div}\mathbb{T}, \qquad (t,x) \in (0,T)\times U, \tag{126}$$

$$\operatorname{div}\boldsymbol{u} = 0$$

$$\mathbb{T} = -p\mathbb{I} + 2\rho\nu\mathbb{D}$$

Where domain $U \subset \mathbb{R}^N$, $N = 2, 3$. These equations must be complemented by boundary conditions (BC). We will only consider the following three types of BC:

- Dirichlet for velocity: $\boldsymbol{u}|_{\Gamma_\mathrm{D}} = \boldsymbol{u}_D$,
- Natural outflow: $\mathbb{T}|_{\Gamma_\mathrm{out}}\,\boldsymbol{n} = 0$,
- Periodic: $\boldsymbol{u}(\boldsymbol{x},t) = \boldsymbol{u}(\boldsymbol{x}+\boldsymbol{L},t)$, $p(\boldsymbol{x},t) = p(\boldsymbol{x}+\boldsymbol{L},t)$ for $x \in \Gamma_\mathrm{periodic}$

where $\boldsymbol{n}$ is the outer surface normal of U and $\boldsymbol{L}$ is a fixed vector mapping one part of a periodic boundary to another[29]. The weak formulation then follows using the standard procedure of multiplying (126) by a test function $\boldsymbol{v}$ (that vanishes on Γ_D) and by integrating in space, which yields:

$$\int_U \left\{ \frac{\partial \boldsymbol{u}}{\partial t}\cdot\boldsymbol{v} + (\nabla\cdot\boldsymbol{u})\,\boldsymbol{u}\cdot\boldsymbol{v} + \frac{1}{\rho}\mathbb{T} : \nabla\boldsymbol{v} - \boldsymbol{f}\cdot\boldsymbol{v} \right\} \mathrm{d}x = 0. \tag{127}$$

(Using integration by parts. The boundary term vanishes for any combination of the three types of BC above.) Similarly, the continuity equation is replaced by

$$\int_U q \operatorname{div}\boldsymbol{u}\,\mathrm{d}x = 0 \tag{128}$$

To solve the weak formulation of Navier-Stokes equations is to find $\boldsymbol{u} : (0,T) \to \boldsymbol{u}_0 + \mathcal{V}$ and $p : (0,T) \to \mathcal{P}$, such that (127), (128) hold for every $\boldsymbol{v} \in \mathcal{V}$ and every $q \in \mathcal{P}$ at almost every $t \in (0,T)$. Here, $\mathcal{V}$ is a *velocity test function space* and $\mathcal{P}$ is the *pressure test function space*. Natural choice of these spaces is:

$$\mathcal{V} = \left\{ \boldsymbol{\phi} \in W^{1,2}(U)^N, \quad \boldsymbol{\phi}|_{\Gamma_D} = 0, \quad \boldsymbol{\phi} \text{ satisfies periodic BCs} \right\},$$
$$\mathcal{P} = L^2(U).$$

[29] This is applicable in case of a rectangular domain.

For more details, see [7]. In numerical computations, we need to make a discretization of both space and time. Regarding the former, we choose a fixed time step τ and replace the time derivative by a difference (implicit Euler)

$$\frac{\partial \boldsymbol{u}}{\partial t} \mapsto \frac{\boldsymbol{u}^n - \boldsymbol{u}^{n-1}}{\tau}, \tag{129}$$

where $\boldsymbol{u}^n$ stands for $\boldsymbol{u}(n\tau)$, $n = 0, 1, 2, \ldots, N$, $T = n\tau$. Regarding the latter, we find finite dimensional spaces $\mathcal{V}_h, \mathcal{P}_h$:

$$\mathcal{V}_h \approx \mathcal{V}, \qquad \mathcal{P}_h \approx \mathcal{P}$$

and solve iteratively for $\boldsymbol{u}^n \in \boldsymbol{u}_0 + \mathcal{V}_h$, $p \in \mathcal{P}_h$ satisfying

$$\int_U \left\{ \left(\frac{\boldsymbol{u}^n - \boldsymbol{u}^{n-1}}{\tau} \right) \cdot \boldsymbol{v} + (\nabla \cdot \boldsymbol{u}^n)\, \boldsymbol{u}^n \cdot \boldsymbol{v} + \frac{1}{\rho} \mathbb{T}^n : \nabla \boldsymbol{v} - \boldsymbol{f}^n \cdot \boldsymbol{v} \right\} \mathrm{d}x = 0. \tag{130}$$

$$\int_U q \operatorname{div} \boldsymbol{u}^n = 0 \tag{131}$$

for every $\boldsymbol{v} \in \mathcal{V}_h$, every $q \in \mathcal{P}_h$ and $n = 1, 2, \ldots N$ (where, of course, $\boldsymbol{u}^0$ is given by the initial condition, $\boldsymbol{f}^n$ stands for $\boldsymbol{f}$ at time $n\tau$ and $\mathbb{T}^n = \mathbb{T}(\boldsymbol{u}^n, p^n)$). We then solved equations (130), (131) via the *FEniCS* software. For the construction of $\mathcal{V}_h, \mathcal{P}_h$ we used the standard Taylor-Hood elements and the finite element mesh generator *Gmsh*.

5.2 Simulation 1: Simplified model

In the subsection (4.3) we discussed a two-dimensional simplification of the problem, where the complex geometry was replaced by a thin shell between two concentric cylinders. There, we assumed an inflow which varied with θ, such that the cosine moment of $|v_z|$ was positive. The problem has been solved analytically using the assumption of irrotationality with respect to θ, z under which the Bernoulli's law can be applied. This assumption, however, is difficult to justify[30]. It can be therefore interesting to study this problem also numerically for a fluid with non-zero vorticity. To this end, let the domain be a rectangle

$$U = (-\pi R, \pi R) \times (-l, 0).$$

The boundary of this domain consists of four sides: Γ_{up}, Γ_{left}, Γ_{right}, Γ_{down}. We consider the following boundary conditions:

[30]Note that the shape of the inflow was assumed to be the result of viscous forces and this is already beyond the applicability of Bernoulli's law

- $\boldsymbol{u} = \boldsymbol{u}_{\text{in}}$ at Γ_{up},
- periodic BC at Γ_{left}, Γ_{right},
- natural outflow BC at Γ_{down},

where

$$\boldsymbol{u}_{\text{in}} = \begin{pmatrix} v_1 \\ -v_2(1+\cos\theta) \end{pmatrix}.$$

Here, v_2 represent the average inflow and v_1 is the speed of precession. For this simulation we have chosen values:

$$v_1 = 0.5 \text{ dm/s}, \quad v_2 = 1 \text{ dm/s}, \quad \nu = 10^{-4} \text{ dm}^2/\text{s}. \tag{132}$$

What we obtain in these experiments that an asymmetric pressure field emerges, as predicted in the analytical section. The simulation can be also done for different values of v_1, v_2 as well as for other profiles, e.g a parabolic profile

$$\boldsymbol{u}_{\text{in}} = \begin{pmatrix} v_1 \\ -\frac{v_2}{2}\left(1 - \left(\frac{\theta}{\pi}\right)^2\right) \end{pmatrix}.$$

Of course, being only a two dimensional model, applicability of this simulation is very limited, but, in our opinion, it nicely captures the underlying idea and motivates more complex three dimensional models.

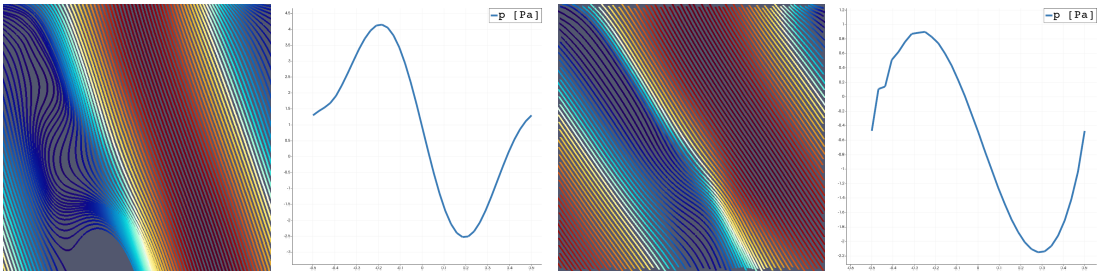

Figure 11: Results of the numerical simulation: the streamlines and the pressure distribution at $z = 0$. Within this simplified model, power on the rotor is proportional to the negative sine moment of this function. First two images correspond to the cosine inlet, the last two are for the parabolic inlet.

5.3 Simulation 2: Three-dimensional model

In order to make a 3d simulation of the turbine, we follow the same strategy used in the section 4: We prescribe a constant speed of precession and then switch into the co-precessing frame, where the geometry appears static. This allows for computations with a fixed mesh, which greatly simplifies the problem. For rotor, we have chosen a truncated conical shape with greatest radius $R_{\text{rot}} = 1.25\,\text{dm}$ and a conical stator of greatest radius $R_{\text{rot}} = 1.35\,\text{dm}$, the Reynolds number was 35283 (this exactly corresponds to parameters in the table (4.2)). Although the geometry is relatively simple, it has a certain bad property and that is the presence of a contact point between the rotor and stator, which is very problematic in terms of mesh generation. Therefore, we decided to crop the geometry by a transversal plane in order to exclude this point. Consequently, the inflow area is an annular region between two circles that are only almost in touch. Of course, the mesh needed to be refined near this narrowed region. Concerning the boundary condi-

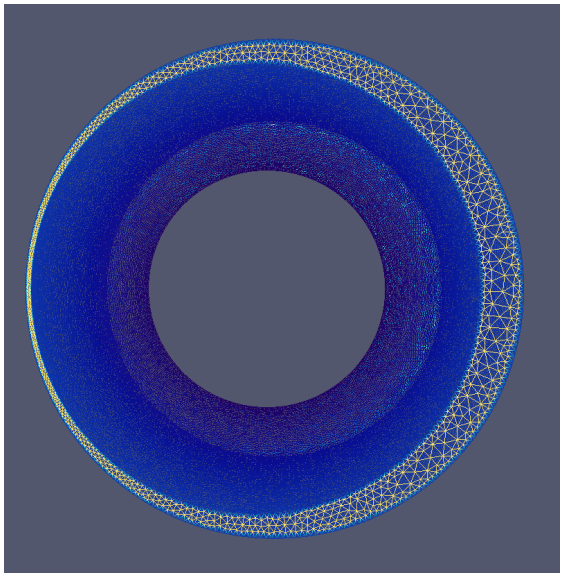

Figure 12: The mesh generated in Gmsh (top view). It is an unstructured mesh made of 172000 tetrahedrons.

tions, we prescribed no-slip at the walls of rotor and stator, Dirichlet inflow at the top and a natural outflow at the bottom. The z-component of velocity at inflow was chosen to be constant[31]. Note that in this simulation, we do not prescribe

[31]We admit that this is problematic from two reasons: Firstly, the exact shape of the velocity profile at the inflow is in fact unknown and secondly, it makes the boundary conditions discontinuous, which reduces stability.

$v_z(r, \theta)$, such that

$$\int_{-\pi}^{\pi} v_z(r, \theta) \cos\theta \, \mathrm{d}\theta < 0.$$

Here, the corresponding condition reads

$$\int_{-\pi}^{\pi} \int_{0}^{R_{\mathrm{stat}}} v_z(r, \theta) \cos\theta \, \mathrm{d}r \, \mathrm{d}\theta < 0$$

where v_z is extended by zero outside the fluid domain. In other words, the average velocity is not necessarily greater in the wider part, but the total flux is. This is satisfied by constant inflow. The output of the simulation was to measure the power on the rotor using formula (76).

The experiment confirmed the existence of drag inversion and also validity of the square law

$$\dot{W} \sim \Omega^2$$

for large values of Ro. In spite of high Reynolds number, the flow appeared to be mostly laminar. However, the simulation became quickly unstable for higher values of Ω. This instability was accompanied with the emergence of backflow near the rear of the rotor. Perhaps, this suggests another mechanism, where orbital motion generates circulation around the rotor in a way similar to a lifting wing — assuming Bernoulli's principle, this circulation should interact with the main flow to generate pressure field and should also contribute to drag inversion. More research and better simulations will be needed to disprove or verify this claim.

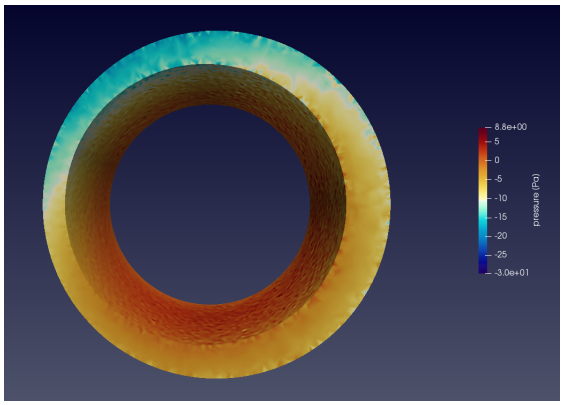

Figure 13: The image depicts the pressure field for very small frequency of rotor precession $f = \Omega/2\pi = 0.2$Hz in a cross section below the point of contact. Regions in red are where the pressure is greatest. The pressure field pushes the rotor upwards (in the positive y direction) in accordance with the direction of orbital movement. Even for this small frequency, the pattern can be clearly recognized.

The following table lists results of four simulations with different values of Ω. In all these simulations, the power stabilized itself after some transition period and this value was used. (The initial state for the simulation was such that the fluid is at rest with respect to the inertial frame). Because of the problems with stability mentioned above, the simulation was done only for suboptimal values of Ω and correspondingly, the power was very low. Nonetheless, the power was positive, indicating that the positive feedback was stronger than friction losses. The table also lists dimensionless parameter c, from the equation

$$c = \frac{\dot{W}}{AQ\Omega^2}.$$

Unfortunately, for an unknown reason, this constant appears to be about ten times smaller than the one from experimental data (which was approximately 0.446, see the table (4.2)). This discrepancy might have been cased by the low rotation rate in our simulations and we shall address it in the future.

f [Hz]	Ω [rad/s]	Ro	$\dot{W}$ [W]	c
0.02	0.126	17.247	2.2e-5	5.33e-2
0.2	1.257	1.725	2.3e-3	5.56e-2
0.5	3.142	0.690	1.4e-2	5.43e-2
1.0	6.283	0.345	4.3e-2	4.16e-2

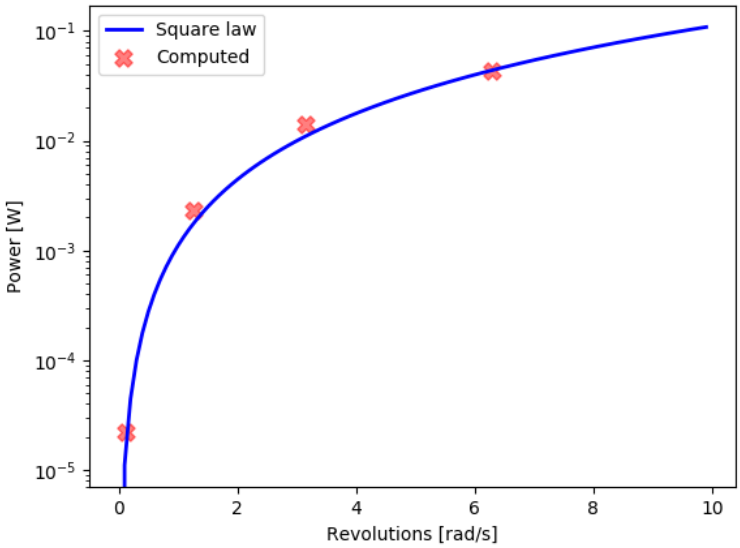

Figure 14: This graph depicts the results of four simulations with different values of Ω. The power follows the square dependence, as predicted by equation (75) with c being roughly constant.

6 Conclusion

To summarize, we developed a simplified analytical model to explain the hydraulic principle behind a rolling turbine (SETUR). This model suggests that a driving fluid force exists as a reaction to the motion of the rotor. This is, in our opinion, atypical in nature, where forces commonly depend on configurational variables, like a position inside an electric field or deflection angle of a pendulum. When force depends on velocity of an object, it usually has dissipative character (friction) or is orthogonal to the direction of the motion and does not perform any work (e.g. the magnetic component of a Lorentz force or the Coriolis force). It seems however, that due to the non-linear behaviour of fluids, it is possible to make a situation where a fluid force depends on the velocity of the rotor and accelerates it. Thermodynamically, this is possible only due to the fact that the system is not closed — there must be a flow which supplies the system with mechanical energy. From a higher perspective, this is how rolling turbines work. Based on our analysis, we also suggested a formula for power in terms of the precession speed Ω and flux Q in the form

$$\dot{W} = \left(a - \frac{b}{|\mathrm{Ro}|} \right) AQ\Omega^2$$

which is in a good agreement with the experimental data and also with the numerics (at least for small Ω). The dependence of power on Ω is in our opinion important, because in future, it could help with choosing appropriate generator for given turbine such that the magnitude of Ω will be optimal. To make such formula practical, we would need to complement it by a formula for hydraulic head[32]

$$H = H(\Omega, Q)$$

and to make some list of geometrical parameters a, b — this could be done in the future[33]. Additional suggestions for further research are:

1. To capture motion of the rotor (especially the transition to the rolling motion) using a high-speed camera.[34]

2. To create a full scale 3d numerical simulation in a deforming geometry using a combination of the co-precessing frame and ALE method.

3. To analyse the possibility of circulation around the rotor (back-flow in the rear of the rotor).

[32] Unfortunately, our strategy was not suitable for deriving this formula.
[33] We should mention that some different formulas for power are also present in [1].
[34] As was also suggested in [8]

7 Appendix: Navier Stokes in Cylindrical Coordinates

We remind that in Cartesian, the incompressible Navier-Stokes equations read as follows:

$$\frac{\partial \mathbf{u}}{\partial t} + (\mathbf{u} \cdot \nabla)\,\mathbf{u} = -\frac{1}{\rho}\nabla p + \nu \Delta \mathbf{u} + \mathbf{f},$$
$$\operatorname{div} \mathbf{u} = 0$$

and that in cylindrical coordinates any point $\mathbf{x}$, which does not lie on the z-axis, is parametrized by variables r, θ, z in a way, which is given by formula

$$\mathbf{x} = \begin{pmatrix} r\,\cos\theta \\ r\,\sin\theta \\ z \end{pmatrix}, \quad r > 0,\ \theta \in \mathbb{R},\ z \in \mathbb{R}.$$

In this framework, it is convenient to define the canonical basis $\mathbf{e}_i$ as

$$(\mathbf{e}_1, \mathbf{e}_2, \mathbf{e}_3) = \left(\hat{r}, \hat{\theta}, \hat{z}\right) = \left(\frac{\partial \mathbf{x}}{\partial r}, \frac{1}{r}\frac{\partial \mathbf{x}}{\partial \theta}, \frac{\partial \mathbf{x}}{\partial z}\right) = \begin{pmatrix} \cos\theta & -\sin\theta & 0 \\ \sin\theta & \cos\theta & 0 \\ 0 & 0 & 1 \end{pmatrix}$$

and differential operators ∂_i as

$$\partial_1 = \frac{\partial}{\partial r}, \quad \partial_2 = \frac{1}{r}\frac{\partial}{\partial \theta}, \quad \partial_3 = \frac{\partial}{\partial z}.$$

Note that $\mathbf{e}_i$ is an orthonormal basis and ∂_i are exactly the directional derivatives $\mathbf{e}_i \cdot \nabla$. Now, our task is to rewrite (15) in terms of ∂_i and components u_i, f_i, given by

$$\mathbf{u} = u_i \mathbf{e}_i, \quad \mathbf{f} = f_i \mathbf{e}_i.$$

In general, the difficulty of curvilinear coordinates arises from the fact that $\mathbf{e}_i$ may vary when $\mathbf{x}$ changes. As a consequence, the differential operators ∂_i do not commute and $\partial_j \mathbf{e}_i$ may be non-zero. To account for the latter, we define the so called *Christoffel symbols* Γ_{ij}^k as the components of vectors $\partial_j \mathbf{e}_i$. That means

$$\partial_j \mathbf{e}_i = \Gamma_{ij}^k \mathbf{e}_k.$$

With this notation, and using orthogonality, the gradient of a vector field $\mathbf{u}$ becomes

$$\nabla \mathbf{u} = [\partial_j \mathbf{u}] \otimes \mathbf{e}_j = [\partial_j (u_i \mathbf{e}_i)] \otimes \mathbf{e}_j = (\partial_j u_i)\,\mathbf{e}_i \otimes \mathbf{e}_j + \Gamma_{ij}^k u_i \mathbf{e}_k \otimes \mathbf{e}_j = u_i|_j\ \mathbf{e}_i \otimes \mathbf{e}_j,$$

where we have introduced the *covariant derivative*

$$u_i|_j = \partial_j u_i + \Gamma^i_{kj} u_k.$$

From here (using orthogonality again), we can quickly see that

$$\operatorname{div} \mathbf{u} = \operatorname{Tr} \nabla \mathbf{u} = u_i|_i$$

and

$$(\mathbf{u} \cdot \nabla)\, \mathbf{u} = \nabla \mathbf{u}(\mathbf{u}) = u_i|_j \, u_j \, \mathbf{e}_i.$$

Finally, the most complicated part is the term $\nu \Delta \mathbf{u}$ which contains second derivatives. For a scalar field φ, we have

$$\begin{aligned} \Delta \varphi = \operatorname{div} (\nabla \varphi) &= \partial_j \left(\partial_i \varphi \, \mathbf{e}_i \right) \cdot \mathbf{e}_j = \partial_{ij} \varphi \, \mathbf{e}_i \cdot \mathbf{e}_j + \partial_i \varphi \, \Gamma^k_{ij} \mathbf{e}_k \cdot \mathbf{e}_j \\ &= \partial_{ii} \varphi + \Gamma^j_{ij} \, \partial_i \varphi \end{aligned}$$

and for a vector field $\mathbf{u}$:

$$\begin{aligned} \Delta \mathbf{u} = \operatorname{div}(\nabla \mathbf{u}) &= \partial_k \left[u_i|_j \, \mathbf{e}_i \otimes \mathbf{e}_j \right] \mathbf{e}_k \\ &= \partial_k \left(u_i|_j \right) (\mathbf{e}_i \otimes \mathbf{e}_j) \mathbf{e}_k + u_i|_j \; \Gamma^l_{ik} \, (\mathbf{e}_l \otimes \mathbf{e}_j) \mathbf{e}_k + u_i|_j \; \Gamma^l_{jk} \, (\mathbf{e}_i \otimes \mathbf{e}_l) \mathbf{e}_k \\ &= \left\{ \partial_j \left(u_i|_j \right) + \Gamma^i_{kj} \;\, u_k|_j + \Gamma^k_{jk} \;\, u_i|_j \right\} \mathbf{e}_i. \end{aligned}$$

Putting everything into (15) and comparing the components, we get a curvilinear version of Navier-Stokes equations:

$$\frac{\partial u_i}{\partial t} + u_i|_j \, u_j = -\frac{1}{\rho} \partial_i p + \nu \left\{ \partial_j \left(u_i|_j \right) + \Gamma^i_{kj} \; u_k|_j + \Gamma^k_{jk} \; u_i|_j \right\} + f_i, \tag{133}$$

$$u_i|_i = 0.$$

So far, we didn't use any particular property of cylindrical coordinates except for local orthogonality. Thus the formula (133) remains valid even for eg. spherical coordinates. Returning to cylindrical, we calculate

$$\frac{\partial \hat{r}}{\partial \hat{\theta}} = \frac{1}{r} \frac{\partial \hat{r}}{\partial \theta} = \frac{\hat{\theta}}{r},$$

$$\frac{\partial \hat{\theta}}{\partial \hat{\theta}} = \frac{1}{r} \frac{\partial \hat{\theta}}{\partial \theta} = -\frac{\hat{r}}{r}.$$

This corresponds to fact that the vectors $\hat{r}$ and $\hat{\theta}$ revolve around the z-axis as θ changes. Hence we have

$$\Gamma^\theta_{r\theta} = \frac{1}{r}, \qquad \Gamma^r_{\theta\theta} = -\frac{1}{r}$$

and it is easy to see that all the remaining components of Γ^j_{ik} are identically zero. Thus the only covariant derivatives, which are not equal to their directional counterparts, are

$$u_r|_\theta = \frac{1}{r}\frac{\partial u_r}{\partial \theta} - \frac{u_\theta}{r}, \qquad u_\theta|_\theta = \frac{1}{r}\frac{\partial u_\theta}{\partial \theta} + \frac{u_r}{r}.$$

Plugging these into (133) and simplifying, we obtain the Navier-Stokes equations in cylindrical coordinates

$$\frac{\partial u_r}{\partial t} + (\partial_j u_r)\, u_j - \frac{u_\theta^2}{r} = -\frac{1}{\rho}\frac{\partial p}{\partial r} + \nu\left\{\partial_{jj} u_r - \frac{2}{r^2}\frac{\partial u_\theta}{\partial \theta} - \frac{u_r}{r^2} + \frac{1}{r}\frac{\partial u_r}{\partial r}\right\} + f_r,$$

$$\frac{\partial u_\theta}{\partial t} + (\partial_j u_\theta)\, u_j + \frac{u_r u_\theta}{r} = -\frac{1}{\rho r}\frac{\partial p}{\partial \theta} + \nu\left\{\partial_{jj} u_\theta + \frac{2}{r^2}\frac{\partial u_r}{\partial \theta} - \frac{u_\theta}{r^2} + \frac{1}{r}\frac{\partial u_\theta}{\partial r}\right\} + f_\theta,$$

$$\frac{\partial u_z}{\partial t} + (\partial_j u_z)\, u_j = -\frac{1}{\rho}\frac{\partial p}{\partial z} + \nu\left\{\partial_{jj} u_z + \frac{1}{r}\frac{\partial u_z}{\partial r}\right\} + f_z.$$

Using scalar material time derivative and Laplace operator:

$$\dot\varphi = \frac{\partial \varphi}{\partial t} + (\partial_j \varphi)\, u_j, \quad \Delta\varphi = \partial_{jj}\varphi + \frac{1}{r}\frac{\partial \varphi}{\partial r}$$

they can be rewritten into a more succinct form

$$\begin{aligned}
\dot u_r - \frac{u_\theta^2}{r} &= -\frac{1}{\rho}\frac{\partial p}{\partial r} + \nu\left\{\Delta u_r - \frac{2}{r^2}\frac{\partial u_\theta}{\partial \theta} - \frac{u_r}{r^2}\right\} + f_r,\\
\dot u_\theta + \frac{u_r u_\theta}{r} &= -\frac{1}{\rho r}\frac{\partial p}{\partial \theta} + \nu\left\{\Delta u_\theta + \frac{2}{r^2}\frac{\partial u_r}{\partial \theta} - \frac{u_\theta}{r^2}\right\} + f_\theta,\\
\dot u_z &= -\frac{1}{\rho}\frac{\partial p}{\partial z} + \nu\Delta u_z + f_z
\end{aligned}$$

and the continuity equation is simply

$$\partial_j u_j + \frac{u_r}{r} = 0.$$

References

[1] F. Maršík, Z. Trávníček. *Performance and efficiency of rolling turbines — theoretical considerations and experimental verification*. 2021, to be published.

[2] L. D. Landau, E. M. Lifshitz. *Fluid Mechanics*. Pergamon Press: Oxford, 1987.

[3] F. Maršík, J. Falta, M. Sedláček. *Theoretical Analysis and Experimental Verification of the Rolling Turbines Performance*. HEFAT2010, 7th International Conference on Heat Transfer, Fluid Mechanics and Thermodynamics, 19-21 July 2010, Antalya, Turkey

[4] Stanislav Hostin, Miroslav Sedláček, Jiří Špidla. *Malý hydroenergetický zdroj, závěrečná správa*. Bratislava, 1997.

[5] Arnold Sommerfeld. *Mechanics of Deformable Bodies*. Academic Press, New York, 1950.

[6] S. Chandrasekhar . *Hydrodynamic and Hydromagnetic Stability*. Clarendon Press, 1961.

[7] V. Girault, P.-A. Raviart. *Finite Element Methods for Navier-Stokes Equations. Theory and Algorithms*. Springer, Berlin, 1986.

[8] Viktoriya Sokalska. *CFD-Analyse und Bewertung einer flügellosen Turbine mit abwälzendem Kegelrotor*. University of Applied Sciences, Düsseldorf, 2009.

[9] Georgy Lebon, David Jou, José Casas-Vázquez. *Understanding Non-equilibrium Thermodynamics*. Springer, 2008.

[10] Martin S. Alnæs and Jan Blechta and Johan Hake and August Johansson and Benjamin Kehlet and Anders Logg and Chris Richardson and Johannes Ring and Marie E. Rognes and Garth N. Wells. *The FEniCS Project Version 1.5*. Archive of Numerical Software, vol. 3, 2015.

[11] A. Logg, K.-A. Mardal, G. N. Wells et al. *Automated Solution of Differential Equations by the Finite Element Method*. Springer, 2012.

[12] A. Logg and G. N. Wells. *DOLFIN: Automated Finite Element Computing*. ACM Transactions on Mathematical Software, vol. 37, 2010.

[13] A. Logg, G. N. Wells and J. Hake Springer. *DOLFIN: a C++/Python Finite Element Library*. 2012.

[14] Michael Turaev. *Numerical Experiments in Billiards.*

[15] V. Beran, M. Sedlaček, F. Maršík. *A new bladeless hydraulic turbine.* Applied Energy 104 (2013) 978-983